

# Multiscale Methods for Computational RNA Enzymology

**Maria T. Panteva\***, **Thakshila Dissanayake\***, **Haoyuan Chen\***,  
**Brian K. Radak\***, **Erich R. Kuechler\***, **George M. Giambaşu\***,  
**Tai-Sung Lee\***, **Darrin M. York<sup>1,\*</sup>**

\*Center for Integrative Proteomics Research, BioMaPS Institute and Department of Chemistry and Chemical Biology, Rutgers University, Piscataway, New Jersey, USA

<sup>1</sup>Corresponding author: e-mail address: york@biomaps.rutgers.edu

## Contents

1. Introduction	336
2. The "Problem Space" of Computational RNA Enzymology	338
3. Multiscale Modeling Strategy	340
4. Catalytic Strategies for Cleavage of the RNA Backbone	340
5. Modeling Ion and Nucleic Acid Interactions	341
5.1 Ion models used in biomolecular simulations	342
5.2 Modeling the ion atmosphere around nucleic acids	343
5.3 Current challenges	345
6. Modeling pH-Rate Profiles for Enzymes	346
6.1 Application to apo and cCMP-bound RNase A	348
6.2 Current challenges	350
7. Modeling Conformational States	351
7.1 Catalytic strategies of ribozymes	352
7.2 General considerations when starting MD simulations from inactive structures	353
7.3 Application to HDVr	354
7.4 Current challenges	356
8. Modeling the Chemical Steps of Catalysis	356
8.1 General considerations	357
8.2 Constructing free energy profiles of HDVr	358
8.3 Current challenges	360
9. Computing KIEs to Verify Transition State Structure	361
9.1 Application of KIE on RNase A and Zn <sup>2+</sup> catalytic mechanisms	361
9.2 Current challenges	363
10. Conclusions	363
Acknowledgments	364
References	364

## Abstract

RNA catalysis is of fundamental importance to biology and yet remains ill-understood due to its complex nature. The multidimensional “problem space” of RNA catalysis includes both local and global conformational rearrangements, changes in the ion atmosphere around nucleic acids and metal ion binding, dependence on potentially correlated protonation states of key residues, and bond breaking/forming in the chemical steps of the reaction. The goal of this chapter is to summarize and apply multiscale modeling methods in an effort to target the different parts of the RNA catalysis problem space while also addressing the limitations and pitfalls of these methods. Classical molecular dynamics simulations, reference interaction site model calculations, constant pH molecular dynamics (CpHMD) simulations, Hamiltonian replica exchange molecular dynamics, and quantum mechanical/molecular mechanical simulations will be discussed in the context of the study of RNA backbone cleavage transesterification. This reaction is catalyzed by both RNA and protein enzymes, and here we examine the different mechanistic strategies taken by the hepatitis delta virus ribozyme and RNase A.



---

## 1. INTRODUCTION

RNA plays several key roles in cellular function (Garst, Edwards, & Batey, 2011; Guttman & Rinn, 2012), ranging from the regulation of gene expression and signaling pathways to catalysis of important biochemical reactions, including protein synthesis (Schmeing & Ramakrishnan, 2009; D. N. Wilson & Cate, 2012) and pre-mRNA splicing (Hoskins & Moore, 2012; Valadkhan, 2010). Since the discovery that RNA molecules could act as enzymes, the study of the novel catalytic properties of RNA has been an area of intense interest and research (Fedor & Williamson, 2005; Sharp, 2009). These efforts have given birth to the field of ribozyme engineering (X. Chen & Ellington, 2009; Link & Breaker, 2009) and influenced theories into of the origin of life itself (X. Chen, Li, & Ellington, 2007; T. J. Wilson & Lilley, 2009). Ultimately, the elucidation of the mechanisms of RNA catalysis promises to yield a wealth of new insights that will extend our understanding of biological processes and facilitate the design of new RNA-based technologies including allosterically controlled ribozymes that may act as molecular switches (Fastrez, 2009; Suess & Weigand, 2008) in RNA chips and new ultra-sensitive biosensing devices (Penchovsky, 2014).

A detailed understanding of the general strategies whereby molecules of RNA can catalyze chemical reactions, including the factors that regulate their activity, provides guiding principles to aid in molecular design. A deep understanding of mechanism, however, requires an interdisciplinary

approach that integrates both theory and experiment (Kellerman, York, Piccirilli, & Harris, 2014; Rhodes, Réblová, Sponer, & Walter, 2006). Experiments can be designed to probe mechanism, but due to the inherent difficulty of directly observing a transition state, primary experimental observables only indirectly report on mechanism and do not provide an atomic-level picture of catalysis (Al-Hashimi & Walter, 2008; Fedor, 2009; Walter, 2007). Computational approaches, and in particular molecular simulation methods, provide a wealth of molecular-level detail, but are derived from approximate models that, without validation from experiments, are not meaningful (Hashem & Auffinger, 2009; McDowell, Špačková, Šponer, & Walter, 2006). Thus, while experimental structural biology, molecular biology, and molecular biophysics approaches provide critical data about ribozyme mechanisms, the translation of these data into knowledge requires interpretation through theoretical models.

In this chapter, we provide a discussion of the multiscale methods used for computational RNA enzymology. These methods have particular relevance to the study of catalytic riboswitches that combine molecular recognition and binding of an effector molecule with conformational changes in the expression platform that lead to catalysis. Each of these elements is sensitive to environmental conditions, including the specific content of the ionic atmosphere as well as pH. Recently, there have been advances in both computational tools as well as experimental methods that have advanced our understanding of RNA catalysis. The goal of this chapter is to present an overview of the multiscale modeling tools used in computational enzymology, what they are used for, and how they can be connected with experiments. Ultimately, a goal of these efforts is to develop robust computational models that not only aid in the interpretation of experimental data but also provide predictive insight.

This chapter is organized as follows. In the first section, an overview of the multiscale modeling approach is given, along with a discussion of why RNA poses particular computational challenges. The second section describes methods for modeling the ionic environment around RNA as a function of ionic conditions. The third section addresses issues of protonation states as a function of pH. The fourth section describes examination of conformational events required to reach a catalytically active structure, and how this structure evolves along the reaction path. The fifth section examines methods to study the catalytic chemical steps of the reaction once a catalytically active state has been achieved. The sixth section will focus on the calculation of kinetic isotope effects (KIEs) to verify the rate-controlling

transition state structure. Along the way, we will use examples of the catalytic mechanism of the hepatitis delta virus ribozyme (HDVr) and RNase A to illustrate key points.



## 2. THE “PROBLEM SPACE” OF COMPUTATIONAL RNA ENZYMOLOGY

The goal of computational RNA enzymology is to provide a detailed atomic-level description of catalysis that is able to unify the interpretations of a wide range of experiments such that a consensus view of mechanism emerges. Ultimately, the elucidation of mechanism requires consideration of specific chemical reaction pathways through a multidimensional free energy landscape that connects reactants to products while departing from a presumed catalytically competent *active state* (Ensing, De Vivo, Liu, Moore, & Klein, 2006; T.-S. Lee, Radak, Pabis, & York, 2013; Vanden-Eijnden, 2009; Wojtas-Niziurski, Meng, Roux, & Bernèche, 2013). However, the mapping of any given pathway is not meaningful unless one also characterizes the free energy associated with formation of the active state itself, i.e., the probability of finding the system in the active state as a function of experimentally tunable environmental variables such as pH and ionic conditions. The active state will be a function of the RNA conformation, protonation state of key residues, and metal ion binding modes. Together with the catalytic chemical steps, these dimensions define the scope of the “problem space” (Fig. 1) that needs to be explored and characterized.

RNA molecules are highly charged and exhibit a high degree of structural variation that is sensitive to the protonation state of nucleobase residues as well as the binding of metal ions and, in the case of riboswitches, small molecules (Bevilacqua, Brown, Nakano, & Yajima, 2004; Draper, 2008; Roth & Breaker, 2009). Other factors involving greater complexity, such as the binding of proteins and intermolecular interactions that occur in macromolecular assemblies, also influence RNA structure and function, but are beyond the scope of the present discussion.

In the case of ribozymes, protonation state and metal ion binding, in addition to being important to achieve a catalytically active conformation, may also play a role in the chemical steps of the reaction. Divalent metal ions (usually  $Mg^{2+}$ ) are universally important for folding under physiological conditions (Grilley, Soto, & Draper, 2006; Misra & Draper, 2002) and, in ribozymes, have been implicated in many instances as directly participating in catalysis (J. Chen et al., 2013; Wong & York, 2012). This makes their roles in folding and catalysis difficult to untangle (Gong, Chen, Bevilacqua, Golden, & Carey, 2009;

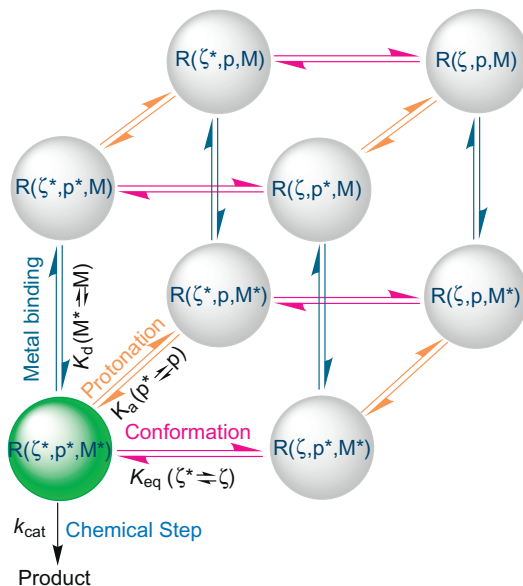
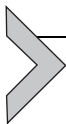


**Figure 1** Complexity of the ribozyme (R) “problem space” involving metal ion interactions/metal binding (M), protonation state (p), and conformational state ( $\zeta$ ) coordinates that lead to a catalytically “active state” (green (dark gray in the print version)). Other variables that represent binding of small molecules and interaction with proteins or other macromolecules are not illustrated. Substrate binding is also not shown, as the primary application focus here is on small self-cleaving RNA enzymes.

Gong, Chen, Yajima, et al., 2009; Misra & Draper, 1998). Similarly, the structure and energetics of RNA, in particular tertiary interactions, are sensitive to pH (Murray, Dunham, & Scott, 2002; Nixon & Giedroc, 2000; Wadkins, Shih, Perrotta, & Been, 2001), as are the catalytic protonation state requirements of key active site residues in ribozymes (Butcher & Pyle, 2011; Doudna & Cech, 2002). The duality of influence of protonation state and metal ion binding on RNA structure and catalytic activity is further complicated by the fact that they are often coupled. Metal ion binding can perturb the  $pK_a$  values of active site residues such that they can be more effective as general acids or bases under physiological conditions, and conversely, ionization events can adjust the occupation of nearby metal binding sites.

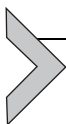
In what follows, we outline a multiscale modeling strategy that takes a “divide-and-conquer” approach to deconstructing the problem space for RNA catalysis using different computational methods. We then go on to give examples of the use of these methods in application to RNA backbone cleavage transesterification reactions catalyzed by a protein and an RNA enzyme that employ two different mechanisms.



### 3. MULTISCALE MODELING STRATEGY

Multiscale simulations involve the integration of a hierarchy of models that, used together, can solve problems that span multiple spatial and/or temporal scales (Dama et al., 2013; Feig, Karanicolas, & Brooks, III, 2004; Lodola & Mulholland, 2013; Meier-Schellersheim, Fraser, & Klauschen, 2009; Sherwood, Brooks, & Sansom, 2008; van der Kamp & Mulholland, 2013; York & Lee, 2009). In the context of biocatalysis, this implies consideration of the enzyme, along with its substrate and any required cofactors, acting in a realistic condensed-phase environment. The active site, where chemical bond formation or cleavage occurs, generally requires a computationally intensive quantum mechanical (QM) description (Garcia-Viloca, Gao, Karplus, & Truhlar, 2004; Hou & Cui, 2013; Lodola & Mulholland, 2013; van der Kamp & Mulholland, 2013; Xie, Orozco, Truhlar, & Gao, 2009), and this problem is amplified by the need for different levels of phase space sampling to capture events that occur on vastly different timescales. Consequently, biocatalysis applications demand the use of multiscale models that can overcome these challenges in a fashion that is both reliable and computationally tractable.

Multiscale modeling simulations of RNA catalysis are laden with challenges that are more pronounced relative to their protein enzyme counterparts (A. A. Chen, Marucho, Baker, & Pappu, 2009; T.-S. Lee, Giambaşu, & York, 2010). The high degree of charge in RNA systems demands careful treatment of electrostatic interactions in the solvated ionic environment, accurate models for ion interactions, and long equilibration times. The increased conformational heterogeneity of RNA relative to typical proteins demands special consideration of sampling in order to get converged structural and thermodynamic properties. The methods used to address these challenges will be described within the context of the example applications that apply them.



### 4. CATALYTIC STRATEGIES FOR CLEAVAGE OF THE RNA BACKBONE

We will focus on cleavage of the phosphodiester backbone of RNA, a fundamental reaction in biology that is catalyzed by protein and RNA enzymes. Studying protein and RNA enzymes together has been a long-standing strategy for better understanding biocatalysis at a fundamental level

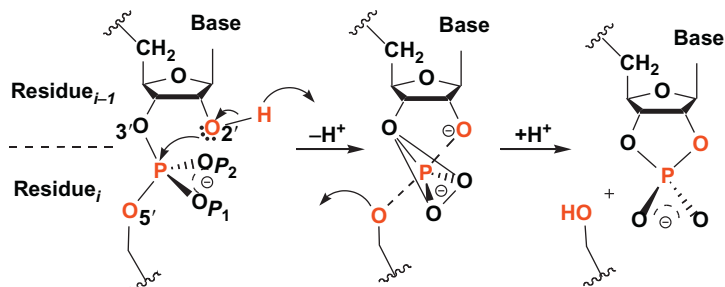
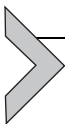


**Figure 2** Reaction schematic of RNA 2'-O-transesterification. The  $O_{2'}$  nucleophile is activated via loss of a proton to a general base and undergoes inline attack on phosphorous to form a pentacoordinate transition structure, followed by departure of the  $O_{5'}$  leaving group which is facilitated by proton donation from a general acid.

(Doudna & Lorsch, 2005) since protein catalysts are composed of a diverse set of amino acid side chains while ribozymes only have four similar nucleobase building blocks to work with. Here, we apply a multiscale modeling approach in the context of a prototype protein enzyme, RNase A, and HDVr which belongs to the class of small self-cleaving nucleolytic ribozymes. RNase A and HDVr catalyze the same phosphoryl transfer reaction via general acid/base mechanisms (Lilley, 2011a, 2011b) (Fig. 2) and require one or more nucleobase or amino acid residues to be in a nonstandard protonation state for catalytic activity (Gong et al., 2007; Wilcox, Ahluwalia, & Bevilacqua, 2011). Enzymes belonging to the RNase superfamily degrade single-stranded RNA specifically, and bovine pancreatic RNase A has been a model enzyme system for studying protein structure and catalytic mechanism for decades (Herschlag, 1994). The HDVr is involved in, and essential for, the rolling-circle replication of the human pathogen, the hepatitis D virus (HDV) where its role is to self-cleave the replicated RNAs into unit length (Ferré-D'Amaré, Zhou, & Doudna, 1998). For RNase A, two histidine residues, His12 and His119, are the proposed general acid and base, respectively (Raines, 1998), while in the case of the HDVr, a  $Mg^{2+}$  ion has been directly implicated in catalysis as the general base, with C75 playing the role as the general acid (Das & Piccirilli, 2005; Gong, Chen, Bevilacqua, et al., 2009; Nakano, Chadalavada, & Bevilacqua, 2000).



## 5. MODELING ION AND NUCLEIC ACID INTERACTIONS

The first dimension in the computational RNA enzymology “problem space” (Fig. 1) refers to metal ion interactions with RNA. The

structure and function of RNA are strongly influenced by interactions with metal ions in solution. These interactions range from tight, specific site binding of divalent metal ions to diffuse territorial binding of monovalent ions in the ion atmosphere around the RNA. Here we provide a brief overview of the most commonly applied ion models used in biomolecular simulations and highlight recent developments in the application of integral equation theories and their relation to recent “ion counting” experiments.

### 5.1. Ion models used in biomolecular simulations

The most commonly used force fields for simulating nucleic acid systems are based on nonpolarizable pairwise potential models (Case et al., 2014; Cornell et al., 1995; Foloppe & MacKerell, Jr., 2000; Jorgensen, Maxwell, & Tirado-Rives, 1996; Kaminski, Friesner, Tirado-Rives, & Jorgensen, 2001; MacKerell, Jr. & Banavali, 2000; Oostenbrink, Villa, Mark, & van Gunsteren, 2004; Pérez et al., 2007; Wang, Cieplak, & Kollman, 2000; Zgarbová et al., 2011) which gain tremendous advantage in computational efficiency at the expense of neglecting explicit many-body quantum effects that are known to be important for many problems (Anisimov, Lamoureux, Vorobyov, Roux, & MacKerell, Jr., 2005; Ponder et al., 2010). Ion parameters are typically parameterized to reproduce bulk properties such as solvation free energies, first shell ion–water distances, and water exchange barriers. For monatomic ions that lack internal conformational degrees of freedom, the main consideration for obtaining correct bulk properties involves balancing the ion–water and ion–ion interaction parameters.

Early monovalent ion parameters that were not properly balanced were found to form aggregated clusters in simulations of various salts in aqueous solution (Auffinger, Cheatham III, & Vaiana, 2007; A. A. Chen & Pappu, 2007). Joung and Cheatham subsequently derived new monovalent ion parameters that considered multiple experimental properties that included structure, dynamics, and solvation, and in addition, salt crystal lattice energies that were sensitive to the cation–anion interactions (Joung & Cheatham III, 2008). This led to a new set of alkali and halide monovalent ion parameters that corrected the “salting out” artifacts of some previous models, but because the ion–ion and ion–water interactions needed to be balanced, it was necessary that separate sets of ion parameters be developed for specific water models. Nonetheless, these parameter sets provided a necessary advance that allowed simulations of nucleic acids to be more reliably extended to longer time domains.

Progress in the development of divalent metal ion models is more challenging, but has nonetheless been the focus of considerable recent effort (Babu & Lim, 2006; Li & Merz, Jr., 2014; Li, Roberts, Chakravorty, & Merz, Jr., 2013; Martínez, Pappalardo, & Marcos, 1999). Recently, a  $\text{Mg}^{2+}$  ion model has been developed for biomolecular simulations that correctly reproduces the ion–water coordination and inner sphere water exchange barrier in solution (Allnér, Nilsson, & Villa, 2012), but that does not necessarily accurately predict absolute solvation thermodynamics (Panteva, Giambaşu, & York, n.d.). More recently, Li et al. (2013) have developed a series of water model-dependent “12–6” models for divalent metal ions that primarily target a single experimental observable. Unlike the monovalent ion parameters, however, the 12–6 divalent metal ion parameters cannot simultaneously reproduce both structural and thermodynamic properties at the same time, owing largely to the neglect of the electronic polarization energy of waters in the first coordination sphere. Follow-up work by the same authors (Li & Merz, Jr., 2014) then introduced “12–6–4” divalent metal ion parameters that make use of a pairwise potential that includes the contribution of the charge-induced dipole interaction in the form of an additional  $r^{-4}$  term added to the traditional Lennard-Jones potential. These divalent ion models have been shown to simultaneously reproduce multiple different properties (Li & Merz, Jr., 2014; Panteva et al., n.d.).

The result of these efforts clearly illustrates the need to create models for metal ions with properly balanced ion–ion and ion–water interactions in order to accurately model bulk properties. In the case of biomolecular simulations involving RNA, these models need to be extended so that the ion–RNA interactions are similarly balanced. The effort to create new models for metal ion interactions with RNA is still in its infancy, owing largely to the fact that there currently is a paucity of quantitative experimental binding and competition data that is amenable to robust force field parameterization efforts. Nonetheless, there has been some preliminary progress in the modeling of the ion atmosphere around nucleic acids, and our recent contributions to this area are described in the next section.

## 5.2. Modeling the ion atmosphere around nucleic acids

The most common approaches to study the distribution of ions around nucleic acids include explicit solvent MD simulations, the three-dimensional reference interaction site model (3D-RISM) (Beglov & Roux, 1997; Kovalenko & Hirata, 2000; Kovalenko, Ten-no, & Hirata, 1999), or through

solving the nonlinear Poisson–Boltzmann (NLPB) equation (Bai et al., 2007; Bond, Anderson, & Record, Jr., 1994; Chu, Bai, Lipfert, Herschlag, & Doniach, 2007; Draper, 2008; Kirmizialtin, Silalahi, Elber, & Fenley, 2012; Pabit et al., 2009). Until recently, solving the NLPB equation was the most common way reported in the literature to study the ion atmosphere surrounding nucleic acids, providing solvation thermodynamics as well as three-dimensional ion distributions. NLPB calculations are simple and computationally efficient, but are limited in the treatment of water as a uniform dielectric and neglect explicit ion–ion correlation. Thus, there is compelling evidence that conventional NLPB does not accurately model the ion atmosphere around nucleic acids (Giambaşu, Luchko, Herschlag, York, & Case, 2014). Methods that consider explicitly the role of water and the correlations between ions, such as 3D-RISM and molecular dynamics simulations with explicit solvent, have only recently become practical to study such problems (A. A. Chen, Draper, & Pappu, 2009; Giambaşu et al., 2014; Luchko et al., 2010; Yoo & Aksimentiev, 2012).

Molecular dynamics simulations, from a theoretical perspective, offer the most rigorous description of solvent structure and dynamics. These simulations, however, are extremely costly and require consideration of very large system sizes (A. A. Chen, Draper, & Pappu, 2009; Giambaşu et al., 2014; Yoo & Aksimentiev, 2012) and long timescales for ion equilibration (Rueda, Cubero, Laughton, & Orozco, 2004; Thomas & Elcock, 2006). Further, solvation thermodynamics is extremely difficult to extract from these calculations. 3D-RISM calculations, on the other hand, integrate out the solvent degrees of freedom and thus allow direct access into solvation thermodynamics, and are sufficiently fast (for fixed solute configurations) that a wide range of ionic conditions can be examined. 3D-RISM calculations can also efficiently explore low salt concentrations (e.g.,  $\mu\text{M}$ – $\text{mM}$  range) where MD suffers from convergence issues that require very long equilibration times and more sophisticated enhanced sampling methods. 3D-RISM calculations are thus potentially very powerful as tools to study the ion atmosphere for nucleic acid systems that can be represented by a relatively small ensemble of rigid conformations. Both MD and 3D-RISM use molecular force fields and, unlike NLPB, yield similar layered solvent and ion distributions (Giambaşu et al., 2014; Howard, Lynch, & Pettitt, 2011; Maruyama, Yoshida, & Hirata, 2010; Yonetani, Maruyama, Hirata, & Kono, 2008) (Fig. 3). A challenge for both 3D-RISM calculations and MD simulations that has been fully recognized only recently (A. A. Chen, Draper, & Pappu, 2009; Giambaşu et al., 2014;

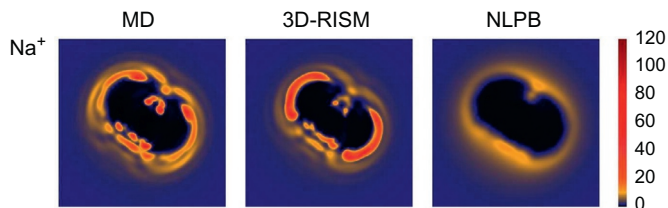


**Figure 3** Comparison of ion distributions around a 24-mer of duplex B-DNA from MD simulation, 3D-RISM, and conventional NLPB. Distributions are shown along a rotating “untwisted” coordinate frame along the DNA axis as described in [Giambaşu et al. \(2014\)](#). Shown are the untwisted  $\text{Na}^+$  densities from MD, 3D-RISM, and NLPB for 0.17 M bulk NaCl concentration. MD and 3D-RISM predict a layered  $\text{Na}^+$  density, whereas NLPB is unstructured.

[Yoo & Aksimentiev, 2012](#)) is the need to consider a sufficiently large amount of solvent such that regions far from the solute exhibit bulk behavior. This is particularly important when comparisons are to be made with experiments that are being performed under different ionic conditions, and thus it is necessary to know what bulk salt concentration the simulations are in equilibrium with.

Recently, several experimental methods have been developed to examine the nature of ion atmosphere around nucleic acids through *ion counting* (IC) experiments that rely on anomalous small-angle X-ray scattering ([Andresen et al., 2004, 2008](#); [Pabit et al., 2010](#); [Pollack, 2011](#)), buffer equilibration atomic absorption spectroscopy ([Bai et al., 2007](#); [Greenfeld & Herschlag, 2009](#)), and titration with fluorescent dyes ([Grilley et al., 2006](#)). In previous decades,  $^{23}\text{Na}$  or  $^{59}\text{Co}$  NMR relaxation rates have also been employed ([Bleam, Anderson, & Record, Jr., 1980](#); [Braunlin, Anderson, & Record, Jr., 1987](#)). IC experiments are important as they quantitatively report directly on the contents of the ion atmosphere around nucleic acids and therefore can be used to facilitate the development of new models. The key observable that allows comparison with experiment is the preferential interaction parameter ( $I$ ) that is, at the microscopic level, an integral measure of the perturbation of the local density of solution components by the highly charged nucleic acid. We have recently reproduced a series of IC measurements using MD simulations, 3D-RISM, and NLPB calculations ([Giambaşu et al., 2014](#)) (Fig. 4).

### 5.3. Current challenges

The difficulties in modeling ion–nucleic acid interactions molecular mechanically are more pronounced when divalent metal ions are involved.

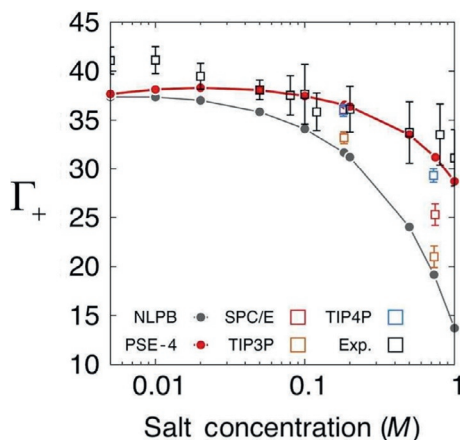
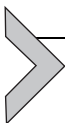


**Figure 4** Ion counting profiles for  $\text{Na}^+$  from MD, 3D-RISM, and NLPB. Data from [Bai et al. \(2007\)](#).

Although experimental IC data are available for divalent metal ions, MD simulations are challenging due to the very slow exchange rates of waters and ligands in the first coordination sphere, and generally slower equilibration timescales. It is likely that enhanced sampling methods will have to be developed in order to extend the scope of MD simulations that can be directly compared with IC experiments. 3D-RISM calculations, on the other hand, are made challenging with applications to divalent metal ions due to convergence issues that arise from the nonlinear equations that need to be solved. These are also influenced by the specific “closure relation” that is applied, and can lead to quantitatively different predicted preferential interaction parameters ([Giambaşu et al., 2014](#)). Consequently, there are technical challenges that need to be met before MD simulations and 3D-RISM calculations can be widely tested and applied to divalent metal ion interactions with nucleic acids, and new models to emerge.



## 6. MODELING pH-RATE PROFILES FOR ENZYMES

The second dimension in the computational RNA enzymology “problem space” ([Fig. 1](#)) involves examination of protonation states. Within the context of catalysis, the specific protonation states of key residues are a critical requirement of the catalytically active state. For general acid/base catalysis, such as in RNase A and HDVr, the general base must

be in the deprotonated form (able to accept a proton) whereas the general acid must be in the protonated form (able to donate a proton) for catalytic activity.

In the analysis of kinetic data as a function of pH, the simplest mechanistic assumption is that the catalytic rate is directly proportional to the probability of the general acid and base being in the active state (Herschlag, 1994). If this assumption is true, and if other protonation events within the pH range of interest are benign with respect to affecting the rate, then general acid/base catalysts will give a classic bell-shaped profile that can be fit to a simple kinetic model where the parameters are the “apparent  $pK_a$ ” values of the general acid and base (Bevilacqua, 2003). Agreement between the kinetic “apparent  $pK_a$ ” values and macroscopic  $pK_a$  values from direct measurements (such as NMR) of the postulated general acid and base is usually considered as evidence in support of their roles in acid/base catalysis. An underlying assumption in this interpretation, however, is that the protonation states of the general acid and base are not correlated (Klingen, Bombarda, & Ullmann, 2006; Ullmann, 2003), i.e., the  $pK_a$  of the general acid is independent of the protonation state of the general base and vice versa. The validity of this assumption, which is system dependent, can be tested computationally in order to gain a more fundamental understanding of catalytic mechanism for a particular system (Dissanayake, Swails, Harris, Roitberg, & York, n.d.).

CpHMD and pH replica exchange molecular dynamics (pH-REMD) have emerged as powerful computational tools for deriving pH-rate profiles for general acid–base catalysts. CpHMD is a method where protonation states are sampled dynamically from a Boltzmann distribution at a fixed pH (Baptista, Martel, & Petersen, 1997; Baptista, Teixeira, & Soares, 2002; Khandogin & Brooks III, 2005; M. S. Lee, Salsbury, Jr., & Brooks III, 2004; Mongan, Case, & McCammon, 2004). We adopt a discrete protonation state model that employs Metropolis Monte Carlo (MC) exchange attempts between different protonation states throughout the course of the MD simulation, (Baptista et al., 2002; Mongan et al., 2004) which has been recently implemented in the AMBER software suite (Mongan et al., 2004) for proteins. Unlike free energy perturbation and thermodynamic integration calculations, CpHMD intrinsically takes into account the correlated effects of residue protonation states for a fixed value of pH. The use of pH-REMD allows multiple simulations to be performed over a range of discrete pH values, and is used to enhance sampling and ensure that simulations are in equilibrium with one another. The

result is that complete atomic-level simulation data, including conditional probabilities for different protonation states (including tautomers), are generated over a range of pH values. From these data, titration and pH-activity curves can be predicted and used to aid in the interpretation of experimental data.

## 6.1. Application to apo and cCMP-bound RNase A

In this section, we apply the CpHMD/pH-REMD method in explicit solvent to RNase A, both in the apo form, and bound to a 2′/3′-cyclic phosphate (cCMP) complex. The simulation data are used to predict the macroscopic and microscopic  $pK_a$  values for the general acid and base, as well as the shape of the pH-rate profile. These results allow us to examine the validity of assumptions about “apparent  $pK_a$ ” values commonly used to interpret experimental pH-rate profiles.

The kinetic model illustrated in Fig. 5 used to interpret pH-rate data in which it is assumed that the functional forms of the general base and acid are  $B^-$  and  $AH^+$ , respectively, and only the active state  $AH^+E_{B^-}$  goes on to give products with a first-order rate constant  $k_{cat}$ . Based on the acid–base equilibrium, there are four different microstates whose probabilities (fractions) are denoted as  $f_{(AH^+/B^-)}$ ,  $f_{(AH^+/BH^-)}$ ,  $f_{(A/BH)}$ , and  $f_{(A/B^-)}$ . The most common and simplest assumption that can be made is that the protonation states of the general acid and base are uncorrelated and can be modeled by “apparent  $pK_a$ ” values for the general acid ( $pK_{a,A}$ ) and base ( $pK_{a,B}$ ), i.e.,  $pK_{a,A} = pK_{a,A}^{BH} = pK_{a,A}^{B^-}$  and  $pK_{a,B} = pK_{a,B}^A = pK_{a,B}^{AH^+}$ . The “apparent  $pK_a$ ” values are determined through fitting to the active fraction  $f_{(AH^+/B^-)}$  and can be compared to the simulated macroscopic  $pK_a$  values obtained from the Hill equation. This procedure is analogous to what is typically done experimentally. Alternately, the full microscopic model in Fig. 5 can be used to fit all the fractions determined from the simulation data. This allows one to assess the degree to which the assumptions inherent in the “apparent  $pK_a$ ”

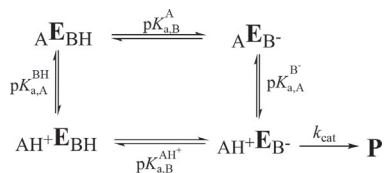


**Figure 5** The microscopic model used in interpretation of pH-rate data. The protonation equilibria between pairwise protonation states are defined in the thermodynamic cycle. The active fraction  $f_{(AH^+/B^-)}$  leads to the products.

model are valid, and to provide a more detailed and direct interpretation of experimental pH-rate data.

The CpHMD/pH-REMD simulations predict macroscopic  $pK_a$  values for His12 and His119 (6.0 and 6.2, respectively) in the apo structure that are quite close to the experimental values (5.8 and 6.2, respectively). The corresponding calculated macroscopic  $pK_a$  values for the cCMP complex (8.5 and 7.3, respectively) are in reasonable agreement with experimental data on 3'-CMP (8.0 and 7.4, respectively). Correspondence of these values with the “apparent  $pK_a$ ” values derived from pH-activity profiles would suggest a mechanistic role for His12 and His119 as the general acid and base.

Figure 6 plots the predicted pH-activity curves (as fractions, or probabilities, for each microstate) from the pH-REMD simulations for RNase A in the apo form and complexed with cCMP. Plotted are the probabilities of the active fractions (red (gray in the print version)) points are from the simulations, and red lines are fitted with the full microscopic  $pK_a$  model illustrated in Fig. 5). Also shown are the fractions for the nonactive states. It is clear

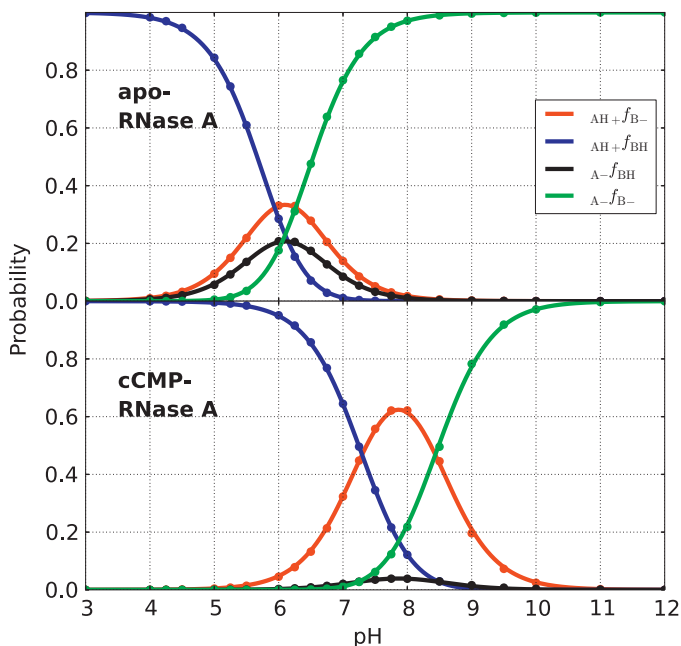


**Figure 6** The pH-activity curves for top: apo-RNase A and bottom: cCMP-bound RNase A. The titratable residues are His12 and His119. The four curves represent the fractions (probabilities) for each of the four possible protonation states, with the red (gray in the print version) curve being the fraction of the catalytically active microstate,  $f_{(AH^+/B^-)}$ .

**Table 1** Experimental and calculated microscopic  $pK_a$ s for apo and cCMP-bound RNase A

	$pK_{a,B}^{AH+}$	$pK_{a,B}^A$	$\Delta pK_{a,B}$	$pK_{a,A}^{BH}$	$pK_{a,A}^{B-}$	$\Delta pK_{a,A}$
<b>apo-RNase A</b>						
Expt. <sup>d</sup>	5.87	6.18	0.31	6.03	6.34	-0.31
Microscopic model	5.94	6.06	0.12	6.15	6.26	-0.12
<b>cCMP-RNase A</b>						
Expt. (3'-UMP) <sup>d</sup>	7.95	7.85	-0.1	6.45	6.35	0.1
Microscopic model	7.30	7.24	-0.06	8.50	8.44	0.06

The calculated microscopic  $pK_a$  values are derived from the thermodynamic cycle illustrated in Fig. 5. The  $\Delta pK_a$  values are the differences in the microscopic  $pK_a$  values and indicate coupling between protonation states (zero  $\Delta pK_a$  values indicate no coupling, as in the “apparent  $pK_a$ ” model).

<sup>d</sup>From Quirk et al. (1999) in order to validate the model.

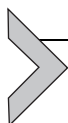
from the figure that the microscopic  $pK_a$  model fits the simulated data extremely well.

Table 1 compares parameters derived from the microscopic model to relevant NMR experiments (Quirk & Raines, 1999). Overall, the calculated and experimental results are quite similar. The general acid and base microscopic  $pK_a$  values (i.e., small  $\Delta pK_a$  values, i.e., less than 0.12 for the simulation results) indicate that the protonation states, in these two examples, are not strongly coupled. This supports the idea that the “apparent  $pK_a$ ” model may be used. Indeed, the “apparent  $pK_a$ ” model gives values of 6.0 and 6.3, respectively, for the apo enzyme, and 8.5 and 7.3, respectively, for the cCMP complex. These are within 0.05  $pK_a$  units of one another. Applying the CpHMD/pH-REMD method in conjunction with fitting the computed pH-activity data with the microscopic model will be particularly useful when general acid and base residues are oppositely charged and in closer proximity in the active site, as is the case with many ribozyme systems.

## 6.2. Current challenges

The ability to accurately compute macroscopic and microscopic  $pK_a$  values of residues involved in acid–base catalysis while at the same time treating effects of correlated protonation states using the CpHMD/REMD method will be an invaluable tool to aid in the interpretation of pH-activity data for catalytic RNAs. This has not yet been demonstrated for RNA systems. It has only been very recently (Goh, Knight, & Brooks III, 2012, 2013) that

models for simulating nucleic acids using CpHMD have been extended to nucleic acids, and they have yet to be thoroughly tested. Challenges that will need to be overcome for application to RNA include consideration of nucleobase tautomers, and coupling of protonation state with divalent metal ion binding (such as has been implicated for HDV<sub>r</sub>). Finally, at this point proton exchange attempts are accepted or rejected based on energies obtained using a Generalized Born (GB) implicit solvation model (Onufriev, Bashford, & Case, 2004), even though the conformational ensembles are generated through MD simulation in explicit solvent. The degree to which this is sufficiently robust for RNA applications has yet to be determined and may need further development.



## 7. MODELING CONFORMATIONAL STATES

The third dimension in the computational RNA enzymology “problem space” (Fig. 1) considers the exploration of thermally accessible conformational states. The characterization of relevant states requires exploration of a vast conformational landscape using accurate models and often specialized methods to enhance sampling. The past few decades have witnessed significant maturation of molecular mechanical (MM) force fields for nucleic acids based on relatively simple fixed charge models and pairwise potentials for nonbonded interactions (Brooks et al., 2009; Pérez et al., 2007; Wang et al., 2000; Zgarbová et al., 2011). The computational efficiency of these models allows MD simulations to routinely access  $\mu$ s timescales (Dror, Dirks, Grossman, Xu, & Shaw, 2012; Salomon-Ferrer, Götz, Poole, Le Grand, & Walker, 2013), making it a viable method for capturing large-scale conformational changes in catalytic riboswitches (Giambaşu, Lee, Scott, & York, 2012; Giambaşu et al., 2010). Taken together, these developments have provided insight into the condensed-phase structure and dynamics of ribozymes both in their precleaved ground state and at various points along a reaction path (T.-S. Lee, Giambaşu, Harris, & York, 2011; T.-S. Lee et al., 2010; T.-S. Lee, Wong, Giambaşu, & York, 2013). Of key importance to the understanding of ribozyme function is to understand what conformational event leads to the catalytically active precleaved ground state, and how does the ribozyme environment respond so as to preferentially stabilize high-energy transition states and intermediates as the reaction progresses. Computational mutagenesis provides insights into the origin of experimental mutational effects on the catalytic rate (T.-S. Lee & York, 2008) and may lead to experimentally testable predictions such as chemical

modifications that test a specific mechanistic hypothesis or correlated mutations that exhibit a rescue effect (T.-S. Lee & York, 2010). In this way, molecular simulations serve as a tool to aid in the interpretation of experimental functional studies and may guide the design of new experiments.

### 7.1. Catalytic strategies of ribozymes

Nucleolytic ribozymes employ a broad range of catalytic strategies for RNA backbone cleavage transesterification (Cochrane & Strobel, 2008; Lilley, 2011a). These may include activation of the nucleophile by a general base, promotion of leaving group departure by a general acid, electrostatic stabilization of the transition state by hydrogen bonding or cationic interactions, and facilitation of proton transfer by Lewis acid activation. However, these are merely general mechanistic considerations that are applicable to many different phosphoryl transfer enzymes (Golden, 2011; Ji & Zhang, 2011). The key question that remains at the heart of our understanding of RNA catalysis is how do certain molecules of RNA, with their relatively limited repertoire of reactive functional groups, adopt three-dimensional conformations that convey catalytic activity that rivals many protein enzymes. Insight into some of these questions may be gleaned from molecular simulations. To date, some general guiding principles have begun to emerge. Current molecular simulation evidence suggests that ribozymes are able to engineer electrostatically strained active sites that can cause shifts of the  $pK_a$  values of key residues or recruit solvent components, including solvent and in some cases divalent metal ions, to assist in catalysis. In the case of the hairpin ribozyme, electrostatic effects in the active site (Nam, Gao, & York, 2008a) account for a large part of the observed rate acceleration and cause a shift of the  $pK_a$  of an adenine nucleobase which acts as a general acid catalyst to facilitate leaving group departure (Nam, Gao, & York, 2008b). The hammerhead ribozyme, on the other hand, has engineered a highly electronegative active site that can recruit a threshold occupation of cationic charge (T.-S. Lee et al., 2009) (a  $Mg^{2+}$  ion under physiological conditions, or multiple monovalent cations under high salt conditions) that facilitates formation of an active in-line attack conformation (T.-S. Lee et al., 2008; T.-S. Lee, Wong, et al., 2013), stabilizes accumulating charge in the transition state, and increases the acidity of the 2'OH group of a conserved guanine residue in order to facilitate proton transfer to the leaving group (Wong, Lee, & York, 2011). In both the hairpin and hammerhead

ribozymes, as well as other ribozymes such as the *glmS* riboswitch (Klein, Been, & Ferré-D'Amaré, 2007; Viladoms, Scott, & Fedor, 2011) and Varkud satellite ribozyme (T. J. Wilson et al., 2010), a guanine is positioned near to the nucleophile and possibly acts as a general base, but its role is still actively debated. In the case of HDVr, the situation appears to be more complex and controversial (Golden, 2011; Nakano, Proctor, & Bevilacqua, 2001). While the HDVr requires divalent metal ions for catalytic activity under physiological conditions, the role of the metal ion, its catalytically active binding mode, and its correlation with other protonation events in the active site are yet to be resolved (Golden, Hammes-Schiffer, Carey, & Bevilacqua, 2013; Lévesque, Reymond, & Perreault, 2012; Wadkins et al., 2001).

## 7.2. General considerations when starting MD simulations from inactive structures

Structural characterization of ribozymes by X-ray crystallography, NMR, and small-angle X-ray scattering have often implicated the involvement of key residues in catalysis based on close proximity to the cleavage site. On departing from these ribozyme structures to run molecular dynamics simulations, however, there are several considerations to take into account. Structures that are not highly resolved, have fractional occupations, or that exhibit a large degree of conformational variation pose difficulties for the computational chemist. Often it becomes necessary to perform many independent MD simulations departing from different starting structures in order to eliminate bias from using a single starting structure.

At the current point in time, the most abundant structural data for ribozymes have been derived from X-ray crystallography (Lilley, 2005; Scott, 2007). These data have been crucial for the field of computational RNA enzymology (Lodola & Mulholland, 2013). Crystal structures must be trapped in a particular state along the reaction path in order to be resolved. Oftentimes, this means deactivating the ribozyme by blocking the nucleophilic  $O_2'$  group by either methylating it or else removing it completely, or by mutating other residues that are known to be critical for activity at different stages along the reaction coordinate. Invariably, these lead to structures that, with respect to the degree to which they represent an active state, are artificial. Ribozymes can also be trapped in transition state mimic structures, such as vanadate (Davies & Hol, 2004) or 2',5'-phosphodiester linkage (Klein et al., 2007; Torelli, Krucinska, & Wedekind, 2007), at the

cleavage site. One must further consider the effect of the crystalline environment as RNA structures can be influenced by crystal packing artifacts that are sensitive to crystallization conditions (Auffinger, Bielecki, & Westhof, 2004; Ennifar, Walter, & Dumas, 2003). In general, one must remember that, although X-ray crystal structures provide invaluable data and critical starting points for molecular simulations, they nonetheless represent static pictures of deactivated enzymes in a crystal environment, whereas meaningful biological interpretation of mechanism requires a dynamical picture of active enzymes in solution. In many cases, molecular dynamics crystal simulations are performed in order to aid in the interpretation of crystallographic data and help to separate the effects of chemical modifications and crystal packing environment on the structure and dynamics of the active enzyme in solution (Heldenbrand et al., 2014; Martick, Lee, York, & Scott, 2008).

### 7.3. Application to HDVr

In the case of the HDVr, several different experimental results are available which highlight the importance and challenge of computational modeling. First, to date, no precleavage wild-type HDVr crystallographic structure exists that includes a fully resolved active site. Until recently, the only precleavage HDVr structure available was that of a catalytically inactive C75U mutant, which has a distinctly different active site architecture compared to the wild-type product state (Ferré-D'Amaré et al., 1998; Ke, Zhou, Ding, Cate, & Doudna, 2004). Specifically, in the inactivated mutant ribozyme, U75 is poised to act as the general base while in the postcleavage structure C75 is located in close proximity to the leaving group, suggesting a general acid role (Ferré-D'Amaré et al., 1998). This role is now strongly supported by biochemical studies (Das & Piccirilli, 2005).

Furthermore, in the C75U structures, no resolved divalent ion shows apparently catalytic importance, although biochemical studies support a direct catalytic role for  $Mg^{2+}$ . It has also been suggested that the  $pK_a$  of C75 in the ribozyme environment is anticorrelated with the presence of  $Mg^{2+}$  (Gong et al., 2007) and that C75 protonation is linked to changes in  $Mg^{2+}$  inner-sphere coordination and binding mode (Gong, Chen, Bevilacqua, et al., 2009; Gong et al., 2008). More recently, a wild-type precleavage HDVr structure (via deoxy mutation of U-1) has been resolved to 1.9 Å. This structure includes a resolved  $Mg^{2+}$  ion with water-mediated contacts to a previously unobserved G-U reverse wobble pair in the active site. Unfortunately, much

of the scissile phosphate (and all of the upstream U-1 nucleotide) in this structure is disordered and could not be resolved; instead, it was modeled using analogy to the active site of the HHR (J.-H. Chen et al., 2010). In this modeled active site structure, U-1 is directly coordinated to  $Mg^{2+}$  via both the  $O_{2'}$  nucleophile and a nonbridging oxygen. These structural data, along with recent kinetic studies of G-U reverse wobble mutants (J. Chen et al., 2013; Lévesque et al., 2012), suggest that a  $Mg^{2+}$  ion may be responsible for activating the nucleophile.

We have previously performed a series of MD simulations of HDVr along the reaction path by using the precleaved C75U mutant structure as a starting point (T.-S. Lee et al., 2011). U75 was modeled as C75, and simulations of the reactant state, precursor state (nucleophile deprotonated), early transition state, late transition state, and product state were conducted for 350 ns each. Representative snapshots from the simulations can be found in Fig. 7.

In the inactive mutant structure, a  $Mg^{2+}$  ion was directly coordinating U75:O<sub>4'</sub> while in our simulations a  $Mg^{2+}$  starting in this position would not remain stably bound. Instead, the  $Mg^{2+}$  was restrained to be within

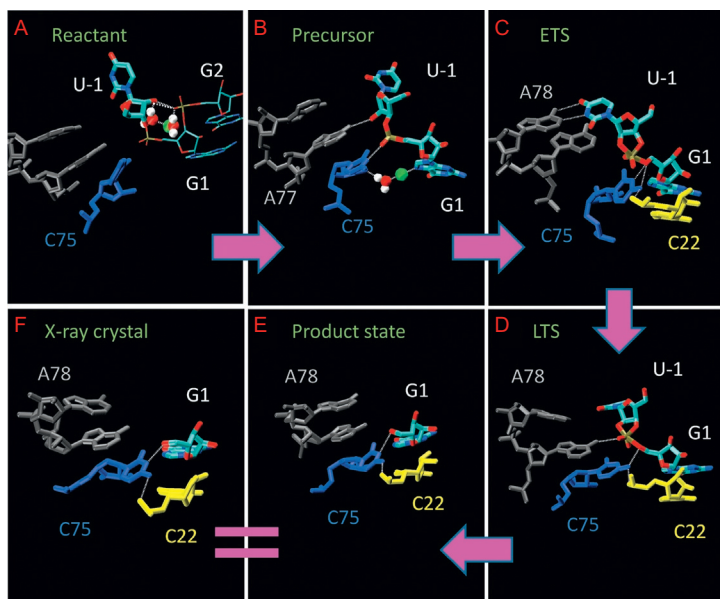


**Figure 7** Representative snapshots taken from simulations of HDVr along the reaction path starting from an inactive C75U mutant crystal structure and compared with the crystal structure of the product state (PDB ID: 1CX0).

2Å of G1:N7 as suggested by J.-H. Chen, Gong, Bevilacqua, Carey, and Golden (2009), and along the reaction path the coordination of this ion in the active site changed. After about 100 ns, the active site of our starting structure for the product state simulation began to converge to the product state crystal structure. This illustrates the importance of running extensive MD simulations to correct for local and/or global conformational changes due to inactive or inaccurate experimental starting structures. Within the context of computational RNA enzymology, one of the main objectives of these MD simulations is to identify a set of plausible catalytically active structure, along with the conformational events that lead to their formation, in order to proceed to the final stage of investigation: to explore the chemical steps of the reaction by testing specific mechanistic hypotheses using QM simulations. This topic will be discussed in the following section.

#### 7.4. Current challenges

Although MD simulation is an increasingly powerful computational tool to study ribozyme mechanism, several limitations exist. The timescales accessible to MD simulations (now on the order of  $\mu$ s) still restricts the types of motions that can be investigated computationally (Dror et al., 2012; Zwier & Chong, 2010). Comprehensive nucleic acid force fields, especially for divalent metal ions, are still being tested and developed and are not as robust as their protein counterparts (Pérez, Luque, & Orozco, 2011). Finally, as mentioned earlier, exploration of the “problem space” of RNA catalysis is complicated by the fact that metal ion interactions, protonation states, and conformational events are intimately coupled, and more progress needs to be made in the development of methods that can efficiently and reliably model this coupling.



## 8. MODELING THE CHEMICAL STEPS OF CATALYSIS

Thus far, we have discussed the use of computational methods to explore the three dimensions of the computational RNA enzymology “problem space” (Fig. 1) in order to arrive at an active state that is competent to proceed on to the catalytic chemical steps of the reaction. It may be the case that more than one plausible active state is identified, and each may have a different probability of being realized under different pH and ionic conditions. To complete the mechanistic picture, it remains to characterize the free energy landscape corresponding to the chemical steps of the

reaction. The individual pathways through this landscape correspond to specific mechanisms, and elucidation of the free energy barriers for each pathway allows prediction of those paths that are most probable. In order to predict reaction kinetics, it is necessary to know the probability of observing the catalytically active state (or more specifically, the precatalytic “reactant” ground state), the pathway, and free energy barrier(s) that connect the reactant state with the product state, as well as other factors (Garcia-Viloca et al., 2004) such as barrier re-crossings and quantum tunneling contributions. In the remainder of this section, we discuss in detail the issue of computing the free energy landscapes and identifying mechanistic pathways for the chemical reaction. This sets the stage for the last section, which is to validate the rate-controlling transition state of a predicted pathway by analyzing KIEs.

Exploration of the free energy landscape for the chemical steps of catalysis where bond formation and cleavage are occurring requires a QM model to describe the changes in electronic structure and energetics. Most enzyme systems are far too large to treat with a fully QM method, although recently advances in so-called linear-scaling quantum force fields may alter that paradigm (Giese, Chen, Huang, & York, 2014; Giese, Huang, Chen, & York, 2014). An attractive alternative that has been widely applied is to use so-called combined QM/MM models (Field et al., 1990; Warshel & Levitt, 1976). These models typically treat a relatively small localized region of the system, such as the key residues in the enzyme active site, with a QM model, whereas the vast remainder of the system is treated with a classical MM force field. QM/MM methods have been widely applied to simulations of enzyme reactions (Acevedo & Jorgensen, 2010; Garcia-Viloca et al., 2004; Senn & Thiel, 2009; van der Kamp & Mulholland, 2013).

### 8.1. General considerations

In QM/MM methods, the first important factor to be considered is the choice of the QM and MM models. The QM method must be accurate to model the reactive chemistry of interest, while also being sufficiently fast to be applied with the required amount of sampling that the application demands. The MM method should be able to reliably model the electrostatic environment surrounding the QM region as well as the relevant conformational events that occur. With a choice of QM and MM models, it then becomes necessary that the QM/MM interaction parameters, and in particular the nonbonded Lennard-Jones potentials, are appropriately balanced so as to give correct energetics. Other specialized terms are required when the boundary between the QM and MM systems occurs across a chemical bond,

and have been described in detail elsewhere (Gao, Amara, Alhambra, & Field, 1998; Reuter, Dejaegere, Maigret, & Karplus, 2000; Y. Zhang, Lee, & Yang, 1999).

Here we will use a fast, approximate semi-empirical quantum model that has been especially designed to accurately model phosphoryl transfer reactions such as those considered in the present work (Nam, Cui, Gao, & York, 2007). This model has been applied previously to examine cleavage transesterification in the hairpin (Nam et al., 2008a, 2008b) and hammerhead (Wong et al., 2011) ribozymes.

Reliable determination of free energy landscapes for enzyme reactions requires sufficient sampling of the generalized coordinates used to define the landscape, in addition to the degrees of freedom orthogonal to the reaction coordinates. A wide range of sampling methods have been developed to overcome these challenges (Zuckerman, 2011). Some of the most widespread include multistage/stratified sampling (Valleau & Card, 1972), statically (Hamelberg, Mongan, & McCammon, 2004; Torrie & Valleau, 1974, 1977) and adaptively (Babin, Roland, & Sagui, 2008; Darve, Rodríguez-Gómez, & Pohorille, 2008; Laio & Parrinello, 2002) biased sampling, self-guided dynamics (Wu & Brooks, 2012), constrained dynamics (Darve & Pohorille, 2001; den Otter, 2000), as well as multicanonical (Berg & Neuhaus, 1992; Nakajima, Nakamura, & Kidera, 1997) and replica exchange (Chodera & Shirts, 2011; Sugita, Kitao, & Okamoto, 2000) algorithms.

Free energy analysis methods need to be incorporated with all simulation data to construct the free energy profile of the reaction coordinates. The weighted histogram analysis method (Kumar, Bouzida, Swendsen, Kollman, & Rosenberg, 1992; Souaille & Roux, 2001) is widely used but requires highly overlapped data and the results are often noisy. The multistate Bennett acceptance ratio (Bennett, 1976; Shirts & Chodera, 2008; Tan, Gallicchio, Lapelosa, & Levy, 2012) methods are broadly applicable but can also suffer from statistical error in the estimation of free energy surfaces when there is low sampling coverage. The recently developed vFEP method uses a general maximum likelihood framework to provide robust analytical estimates to the free energy surface, and offers some advantage over alternative methods (T.-S. Lee, Radak, Huang, Wong, & York, 2014; T.-S. Lee, Radak, et al., 2013).

## 8.2. Constructing free energy profiles of HDVr

In this section, we provide a demonstration application of the calculation of the 2D free energy profile for the general acid step in HDVr catalysis. The goal is to examine the feasibility of a previously proposed mechanistic

hypothesis (J.-H. Chen et al., 2010; Golden, 2011) whereby the catalytic precursor state involves a  $\text{Mg}^{2+}$  ion bound in a bridging position between the scissile phosphate and a phosphate from a neighboring strand. In this position, the divalent ion is able to coordinate the nucleophile and facilitates its activation. The presumed general acid in this mechanism is a protonated cytosine residue (C75).

Figure 8 shows the 2D free energy surfaces, departing from the activated nucleophile, for the reaction in the presence and absence of a bound  $\text{Mg}^{2+}$

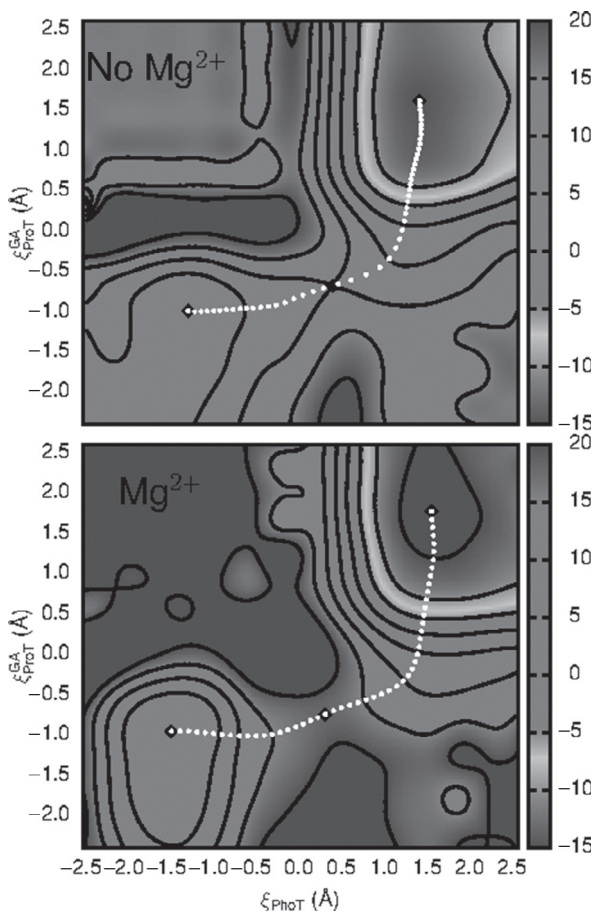


**Figure 8** 2D free energy surfaces for the general acid step of HDVr catalysis departing from a state where the nucleophile has been activated in a prior step. Shown are simulations in the absence (top) and in the presence (bottom) of a  $\text{Mg}^{2+}$  bound in the active site. Minima and saddle points (diamonds) and the minimum free energy path (white points) are also indicated.

ion, henceforth referred to as simply “Mg<sup>2+</sup>” and “no Mg<sup>2+</sup>” simulations. Two reaction coordinates are used to describe the reaction progression:  $\xi_{\text{ProT}}^{\text{GA}}$  is a “general acid proton transfer” coordinate, defined as the difference in distances between the proton and the general acid, and the proton and leaving group;  $\xi_{\text{PhoT}}$  is a “phosphoryl transfer” progression coordinate defined as the difference in distances between the phosphorus and the leaving group, and the phosphorus and the nucleophile.

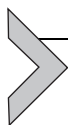
Analysis of the 2D free energy profiles in the presence and absence of a Mg<sup>2+</sup> bound at the active site suggests the minimum free energy pathways are similar, with phosphoryl transfer leading to a late transition state with an almost fully cleaved bond to the leaving group, followed by asynchronous proton transfer from the general acid. Although the mechanistic pathways are similar, the free energy barrier in the absence of Mg<sup>2+</sup> (10.0 kcal/mol) is approximately 8 kcal/mol lower than that for the model where Mg<sup>2+</sup> is present (18.0 kcal/mol), and both of the barriers are considerably lower than the experimental catalytic barrier (estimated to be approximately 19.6–19.8 kcal/mol in the presence of Mg<sup>2+</sup>). The reason for this apparent discrepancy is that one needs to consider the free energy associated with formation of the activated precatalytic state with the nucleophile deprotonated, which was the starting state for the QM/MM calculations. This activation is expected to be considerably less in the presence of the Mg<sup>2+</sup> ion, but it is not yet clear as to whether this is enough to account for the experimental difference. Work to further reconcile these issues is in progress.

Hence, the simulation-derived free energy profiles suggest that based on the proposed mechanistic hypothesis (J.-H. Chen et al., 2010; Golden, 2011), these two cases should have similar mechanisms but the reaction barriers departing from the activated nucleophile are different due to the presence of the proposed active site Mg<sup>2+</sup>. The QM/MM work presented here is therefore not yet conclusive, and ongoing work is needed to characterize the free energy associated with Mg<sup>2+</sup> ion binding, and determine the resulting pK<sub>a</sub> shift on the nucleophile. In addition, alternative competing mechanistic hypotheses that are consistent with experiments should also be explored. Finally, as will be discussed in the next section, once plausible pathways have been determined and the rate-controlling transition state identified, further validation of the pathway can be sought through the measurement and calculation of KIEs.

### 8.3. Current challenges

Computationally tractable methods are needed that allow accurate determination of free energy surfaces using high-level density-functional methods.

Currently, the QM/MM studies that have used density-functional methods for ribozymes have done so with small basis sets (which are notoriously problematic for anionic systems) and either neglected to do any simulation or else employed very short timescales. A promising research direction involves developing methods that allow free energy surfaces generated from exhaustive sampling with low level methods to be systematically corrected to higher levels with significantly reduced sampling requirements. Further, the current models treat the QM/MM interactions as decoupled from the electron density, e.g., they are independent of the local charge. This can lead to overstabilization of anions which are larger, and hence less solvated. Finally, the ability to calculate free energy profiles from linear-scaling quantum force fields is forthcoming and promises to advance the field.



## 9. COMPUTING KIEs TO VERIFY TRANSITION STATE STRUCTURE

KIEs are powerful experimental probes that report directly on properties of the rate-controlling transition state (Cleland & Hengge, 2006; Hengge, 2002). In these experiments, the isotopic mass of one or more atoms involved in the reaction is selectively altered, typically to a heavier isotope. Experiments are then devised to accurately measure the ratio of rate constants corresponding to reactions of the light and heavy isotope ( $KIE = k_{\text{light}}/k_{\text{heavy}}$ ). KIE values that are greater than unity are referred to as “normal,” whereas values less than unity are referred to as “inverse.” Most importantly, KIEs are very sensitive to changes in transition state bonding environment and ultimately encode information about the transition state that allows validation of predicted pathways that pass through it, which in turn provides insight into enzyme mechanism (Harris & Cassano, 2008; Lassila, Zalatan, & Herschlag, 2011). Nonetheless, a detailed interpretation of KIE data in terms of structure and bonding in the transition state requires the use of computational QM models (H. Chen et al., 2014; Wong et al., 2012).

### 9.1. Application of KIE on RNase A and $Zn^{2+}$ catalytic mechanisms

We have recently investigated the mechanistic details of RNase A using a joint experimental and theoretical approach through the determination of experimental KIEs and their interpretation using computational models (Gu et al., 2013). These results are placed into context of baseline

nonenzymatic reaction models (Wong et al., 2012), and models where catalysis is affected by  $\text{Zn}^{2+}$  ions in solution (H. Chen, Harris, & York, n.d.). KIE values for the nucleophile  $\text{O}_2'$ , nonbridging phosphoryl oxygens, and leaving group  $\text{O}_5'$ , designated  $^{18}k_{\text{NUC}}$ ,  $^{18}k_{\text{NPO}}$  and  $^{18}k_{\text{LG}}$ , respectively, were calculated with density-functional QM models (H. Chen et al., n.d.) as well as measured. The results are summarized in Fig. 9.

The nonenzymatic model has a  $^{18}k_{\text{NUC}}$  value near unity and a very large  $^{18}k_{\text{LG}}$  value. The models indicate the transition state is very late (cleavage to the leaving group is almost complete). The reaction catalyzed by RNase A shows a  $^{18}k_{\text{NUC}}$  value that is trending toward being slightly inverse, and the  $^{18}k_{\text{LG}}$  value is significantly reduced. Overall, the models indicate that this corresponds to a late transition state that is overall more compact than

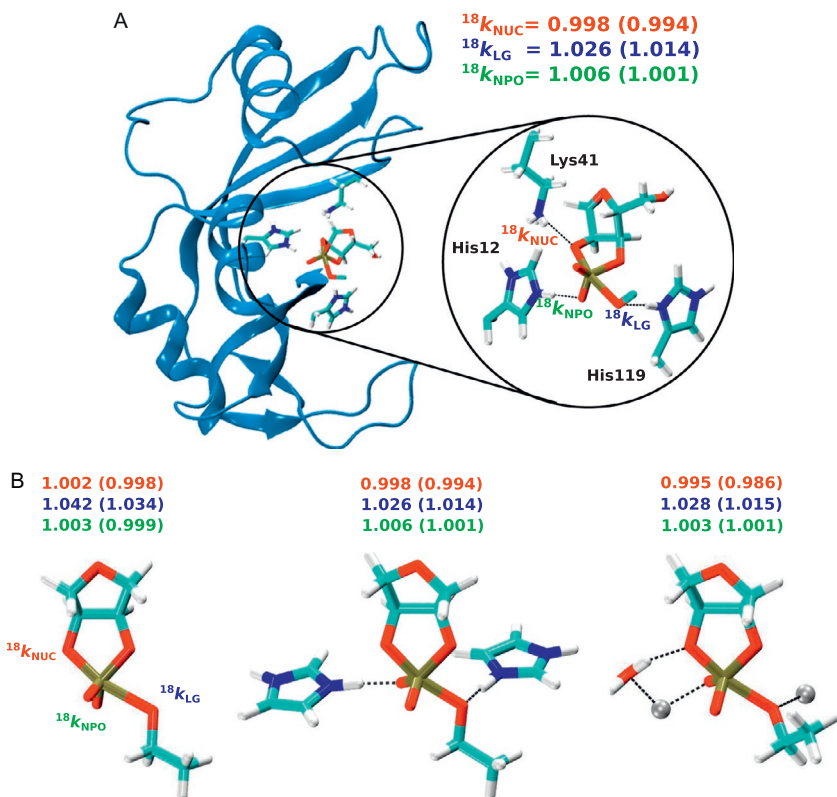


**Figure 9** (A) Snapshot of RNase A transition state mimic structure from MD simulation and (B) transition state geometries and KIEs of nonenzymatic (left), RNase A-catalyzed (middle), and  $\text{Zn}^{2+}$ -catalyzed (right) RNA transphosphorylation model reactions obtained from QM calculations.

the nonenzymatic model reaction. More recently, the KIEs for RNA transphosphorylation catalyzed by  $\text{Zn}^{2+}$  ions in solution have been measured (S. Zhang et al., n.d.). It is of considerable interest that the experimental KIE values for the  $\text{Zn}^{2+}$ -catalyzed reaction are similar to those measured for the reaction catalyzed by RNase A. Further, the computational models for both these reactions that give the closest agreement with experiment are strikingly similar. The  $\text{Zn}^{2+}$  ion positions mimic closely those of the protonated histidine residues for RNase A. A slight difference is that, for the  $\text{Zn}^{2+}$ -catalyzed reaction, there is an additional hydrogen bond to the nucleophile donated from a  $\text{Zn}^{2+}$ -coordinated water molecule. This manifests itself in making the  $^{18}k_{\text{NUC}}$  value slightly more inverse. Overall, these results suggest that the transition states for the catalyzed reactions are altered from that of the nonenzymatic model in a similar fashion by the RNase A enzyme environment or by  $\text{Zn}^{2+}$  ions in solution. Further, the agreement between the experimental and calculated KIE results provides support that the predicted mechanistic pathway for RNase A passes through a late transition state where the interactions illustrated in Fig. 9 are preserved.

## 9.2. Current challenges

At the moment, the calculation of KIEs for large enzyme or ribozyme systems is very tedious and time consuming. The development of computationally more efficient electronic structure methods that were made to be linear scaling and seamlessly integrated into a multiscale modeling framework for the calculation of KIEs would be extremely valuable.



## 10. CONCLUSIONS

In this chapter, we have applied a multiscale modeling strategy to the computational RNA enzymology “problem space” that, for the purposes here, consists of four major modeling components: metal ion–nucleic acid interactions, pH–rate profiles, catalytically active conformations, and the catalytic chemical steps in the reaction. Each of these components has a direct connection with experiment and can be integrated to form a detailed, atomic-level picture of ribozyme mechanism. The ultimate goal of computational RNA enzymology is to provide a unified interpretation of a wide range of experiments that leads to a consensus view of mechanism. Toward this end, a variety of computational methods have been brought to bear on different elements of the problem space.

Classical MD simulations have proven to be instrumental to probe structure and dynamics of ribozymes along their reaction path, as well as providing the most rigorous (although less practical) description of the solvated ionic atmosphere around nucleic acids. Other molecular solvation theory models, such as 3D-RISM, appear very promising as a practical tool to investigate a wide range of ionic conditions for a sufficiently small ensemble of structures. Molecular simulations under conditions of constant pH, together with pH-REMD, can be used to predict and interpret pH-rate profiles for general acid/base catalysts and account for coupling between protonation states that are difficult to probe experimentally. Departing from a presumed active state, QM/MM simulations can be used with enhanced sampling methods such as Hamiltonian replica exchange methods to determine multidimensional free energy landscapes for catalysis. Minimum free energy pathways through these surfaces provide predictions of the specific mechanisms. Predicted mechanisms can be further tested by calculation of KIEs for the rate-controlling transition state along a given path, which can then be verified experimentally. Overall, this field is still rapidly maturing, and much progress is to be expected over the next decade in the development of integrated methods that will allow even closer connections between theory and experiment to be made, and models that provide a predictive understanding of ribozyme mechanism.

## ACKNOWLEDGMENTS

This work was made possible by the National Institutes of Health (NIH) grant numbers P01GM066275 and GM62248 to D. M. Y. and by the National Science Foundation (NSF) CDI type-II grant #1125332 fund to D. M. Y. Computational resources utilized for this research include the Extreme Science and Engineering Discovery Environment (XSEDE), NSF grant number OCI-1053575, the Blue Waters super computer, NSF grant numbers ACI-0725070 and ACI-1238993, and the Minnesota Supercomputing Institute for Advanced Computational Research (MSI).

## REFERENCES

- Acevedo, O., & Jorgensen, W. L. (2010). Advances in quantum and molecular mechanical (QM/MM) simulations for organic and enzymatic reactions. *Accounts of Chemical Research*, 43, 142–151.
- Al-Hashimi, H. M., & Walter, N. G. (2008). RNA dynamics: It is about time. *Current Opinion in Structural Biology*, 18(3), 321–329.
- Allnér, O., Nilsson, L., & Villa, A. (2012). Magnesium ion–water coordination and exchange in biomolecular simulations. *Journal of Chemical Theory and Computation*, 8(4), 1493–1502.
- Andresen, K., Das, R., Park, H. Y., Smith, H., Kwok, L., Lamb, J., et al. (2004). Spatial distribution of competing ions around DNA in solution. *Physical Review Letters*, 93(24), 248103.

- Andresen, K., Qiu, X., Pabit, S. A., Lamb, J. S., Park, H. Y., Kwok, L. W., & Pollack, L. (2008). Mono- and trivalent ions around DNA: A small-angle scattering study of competition and interactions. *Biophysical Journal*, *95*(1), 287–295.
- Anisimov, V. M., Lamoureux, G., Vorobyov, I. V., Huang, N., Roux, B., & MacKerell, A. D., Jr. (2005). Determination of electrostatic parameters for a polarizable force field based on the classical drude oscillator. *Journal of Chemical Theory and Computation*, *1*, 153–168.
- Auffinger, P., Bielecki, L., & Westhof, E. (2004). Anion binding to nucleic acids. *Structure*, *12*, 379–388.
- Auffinger, P., Cheatham, T. E., III, & Vaiana, A. C. (2007). Spontaneous formation of KCl aggregates in biomolecular simulations: A force field issue? *Journal of Chemical Theory and Computation*, *3*, 1851–1859.
- Babin, V., Roland, C., & Sagui, C. (2008). Adaptively biased molecular dynamics for free energy calculations. *Journal of Chemical Physics*, *128*, 134101.
- Babu, C. S., & Lim, C. (2006). Empirical force fields for biologically active divalent metal cations in water. *Journal of Physical Chemistry A*, *110*, 691–699.
- Bai, Y., Greenfeld, M., Travers, K. J., Chu, V. B., Lipfert, J., Doniach, S., & Herschlag, D. (2007). Quantitative and comprehensive decomposition of the ion atmosphere around nucleic acids. *Journal of the American Chemical Society*, *129*(48), 14981–14988.
- Baptista, A. M., Martel, P. J., & Petersen, S. B. (1997). Simulation of protein conformational freedom as a function of pH: Constant-pH molecular dynamics using implicit titration. *Proteins*, *27*, 523–544.
- Baptista, A. M., Teixeira, V. H., & Soares, C. M. (2002). Constant-pH molecular dynamics using stochastic titration. *Journal of Chemical Physics*, *117*, 4184–4200.
- Beglov, D., & Roux, B. (1997). An integral equation to describe the solvation of polar molecules in liquid water. *Journal of Physical Chemistry. B*, *101*, 7821–7826.
- Bennett, C. H. (1976). Efficient estimation of free energy differences from Monte Carlo data. *Journal of Computational Physics*, *22*, 245–268.
- Berg, B. A., & Neuhaus, T. (1992). Multicanonical ensemble: A new approach to simulate first-order phase transitions. *Physical Review Letters*, *68*, 9–12.
- Bevilacqua, P. C. (2003). Mechanistic considerations for general acid-base catalysis by RNA: Revisiting the mechanism of the hairpin ribozyme. *Biochemistry*, *42*, 2259–2265.
- Bevilacqua, P. C., Brown, T. S., Nakano, S., & Yajima, R. (2004). Catalytic roles for proton transfer and protonation in ribozymes. *Biopolymers*, *73*, 90–109.
- Bleam, M. L., Anderson, C. F., & Record, T., Jr. (1980). Relative binding affinities of monovalent cations for double-stranded DNA. *Proceedings of the National Academy of Sciences of the United States of America*, *77*(6), 3085–3089.
- Bond, J. P., Anderson, C. F., & Record, M. T., Jr. (1994). Conformational transitions of duplex and triplex nucleic acid helices: Thermodynamic analysis of effects of salt concentration on stability using preferential interaction coefficients. *Biophysical Journal*, *67*(2), 825–836.
- Braunlin, W. H., Anderson, C. F., & Record, M. T., Jr. (1987). Competitive interactions of  $\text{Co}(\text{NH}_3)_6^{3+}$  and  $\text{Na}^+$  with helical B-DNA probed by  $^{59}\text{Co}$  and  $^{23}\text{Na}$  NMR. *Biochemistry*, *26*(24), 7724–7731.
- Brooks, B. R., Brooks, C. L., III, MacKerell, A. D., Jr., Nilsson, L., Petrella, R. J., Roux, B., et al. (2009). CHARMM: The biomolecular simulation program. *Journal of Computational Chemistry*, *30*(10), 1545–1614.
- Butcher, S. E., & Pyle, A. M. (2011). The molecular interactions that stabilize RNA tertiary structure: RNA motifs, patterns, and networks. *Accounts of Chemical Research*, *44*, 1302–1311.
- Case, D., Babin, V., Berryman, J., Betz, R., Cai, Q., Cerutti, D., et al. (2014). *AMBER 14*. San Francisco, CA: University of California, San Francisco.

- Chen, A. A., Draper, D. E., & Pappu, R. V. (2009). Molecular simulation studies of monovalent counterion-mediated interactions in a model RNA kissing loop. *Journal of Molecular Biology*, 390(4), 805–819.
- Chen, A. A., Marucho, M., Baker, N. A., & Pappu, R. V. (2009). Simulations of RNA interactions with monovalent ions. *Methods in Enzymology*, 469, 411–432.
- Chen, A. A., & Pappu, R. V. (2007). Parameters of monovalent ions in the AMBER-99 forcefield: Assessment of inaccuracies and proposed improvements. *Journal of Physical Chemistry. B*, 111, 11884–11887.
- Chen, H., Giese, T. J., Huang, M., Wong, K.-Y., Harris, M. E., & York, D. M. (2014). Mechanistic insights into RNA transphosphorylation from kinetic isotope effects and linear free energy relationships of model reactions. *Chemistry: A European Journal*, 20, 14336–14343.
- Chen, H., Harris, M. E., & York, D. M. (n.d.). The effect of  $Zn^{2+}$  binding on the mechanism of RNA transphosphorylation interpreted through kinetic isotope effects. *Biochimica et Biophysica Acta*, in press.
- Chen, J., Ganguly, A., Miswan, Z., Hammes-Schiffer, S., Bevilacqua, P. C., & Golden, B. L. (2013). Identification of the catalytic  $Mg^{2+}$  ion in the hepatitis delta virus ribozyme. *Biochemistry*, 52(3), 557–567.
- Chen, J.-H., Gong, B., Bevilacqua, P. C., Carey, P. R., & Golden, B. L. (2009). A catalytic metal ion interacts with the cleavage site GU wobble in the HDV ribozyme. *Biochemistry*, 48, 1498–1507.
- Chen, J.-H., Yajima, R., Chadalavada, D. M., Chase, E., Bevilacqua, P. C., & Golden, B. L. (2010). A 1.9 Å crystal structure of the HDV ribozyme precleavage suggests both Lewis acid and general acid mechanisms contribute to phosphodiester cleavage. *Biochemistry*, 49(31), 6508–6518.
- Chen, X., & Ellington, A. D. (2009). Design principles for ligand-sensing, conformation-switching ribozymes. *PLoS Computational Biology*, 5, 1000620.
- Chen, X., Li, N., & Ellington, A. D. (2007). Ribozyme catalysis of metabolism in the RNA world. *Chemistry & Biodiversity*, 4, 633–655.
- Chodera, J. D., & Shirts, M. R. (2011). Replica exchange and expanded ensemble simulations as Gibbs sampling: Simple improvements for enhanced mixing. *Journal of Chemical Physics*, 135, 194110.
- Chu, V. B., Bai, Y., Lipfert, J., Herschlag, D., & Doniach, S. (2007). Evaluation of ion binding to DNA duplexes using a size-modified Poisson-Boltzmann theory. *Biophysical Journal*, 93(9), 3202–3209.
- Cleland, W. W., & Hengge, A. C. (2006). Enzymatic mechanisms of phosphate and sulfate transfer. *Chemical Reviews*, 106, 3252–3278.
- Cochrane, J. C., & Strobel, S. A. (2008). Catalytic strategies of self-cleaving ribozymes. *Accounts of Chemical Research*, 41, 1027–1035.
- Cornell, W. D., Cieplak, P., Bayly, C. I., Gould, I. R., Merz, K. M., Jr., Ferguson, D. M., et al. (1995). A second generation force field for the simulation of proteins, nucleic acids and organic molecules. *Journal of the American Chemical Society*, 117, 5179–5197.
- Dama, J. F., Sinitskiy, A. V., McCullagh, M., Weare, J., Roux, B., Dinner, A. R., & Voth, G. A. (2013). The theory of ultra-coarse-graining. 1. General principles. *Journal of Chemical Theory and Computation*, 9, 2466–2480.
- Darve, E., & Pohorille, A. (2001). Calculating free energies using average force. *Journal of Chemical Physics*, 115(20), 9169–9183.
- Darve, E., Rodríguez-Gómez, D., & Pohorille, A. (2008). Adaptive biasing force method for scalar and vector free energy calculations. *Journal of Chemical Physics*, 128(14), 144120.
- Das, S., & Piccirilli, J. (2005). General acid catalysis by the hepatitis delta virus ribozyme. *Nature Chemical Biology*, 1(1), 45–52.
- Davies, D. R., & Hol, W. G. J. (2004). The power of vanadate in crystallographic investigations of phosphoryl transfer enzymes. *FEBS Letters*, 577(3), 315–321.

- den Otter, W. K. (2000). Thermodynamic integration of the free energy along a reaction coordinate in Cartesian coordinates. *Journal of Chemical Physics*, 112(17), 7283–7292.
- Dissanayake, T., Swails, J., Harris, M. E., Roitberg, A. E., & York, D. M. (n.d.). Interpretation of pH-rate profiles for acid-base catalysis from molecular simulations., *Biochemistry*, in press.
- Doudna, J. A., & Cech, T. R. (2002). The chemical repertoire of natural ribozymes. *Nature*, 418, 222–228.
- Doudna, J. A., & Lorsch, J. R. (2005). Ribozyme catalysis: Not different, just worse. *Nature Structural and Molecular Biology*, 12(5), 395–402.
- Draper, D. E. (2008). RNA folding: Thermodynamic and molecular descriptions of the roles of ions. *Biophysical Journal*, 95(12), 5489–5495.
- Dror, R. O., Dirks, R. M., Grossman, J. P., Xu, H., & Shaw, D. E. (2012). Biomolecular simulation: A computational microscope for molecular biology. *Annual Review of Biophysics*, 41, 429–452.
- Ennifar, E., Walter, P., & Dumas, P. (2003). A crystallographic study of the binding of 13 metal ions to two related RNA duplexes. *Nucleic Acids Research*, 31(10), 2671–2682.
- Ensing, B., De Vivo, M., Liu, Z., Moore, P., & Klein, M. L. (2006). Metadynamics as a tool for exploring free energy landscapes of chemical reactions. *Accounts of Chemical Research*, 39(2), 73–81.
- Fastrez, J. (2009). Engineering allosteric regulation into biological catalysts. *ChemBiochem*, 10, 2824–2835.
- Fedor, M. J. (2009). Comparative enzymology and structural biology of RNA self-cleavage. *Annual Review of Biophysics*, 38, 271–299.
- Fedor, M. J., & Williamson, J. R. (2005). The catalytic diversity of RNAs. *Nature Reviews. Molecular Cell Biology*, 6, 399–412.
- Feig, M., Karanicolas, J., & Brooks, C. L., III. (2004). MMTSB tool set: Enhanced sampling and multiscale modeling methods for applications in structure biology. *Journal of Molecular Graphics & Modelling*, 22, 377–395.
- Ferré-D'Amaré, A. R., Zhou, K., & Doudna, J. A. (1998). Crystal structure of a hepatitis delta virus ribozyme. *Nature*, 395, 567–574.
- Field, M. J., Bash, P. A., & Karplus, M. (1990). A combined quantum mechanical and molecular mechanical potential for molecular dynamics simulations. *Journal of Computational Chemistry*, 11, 700–733.
- Foloppe, N., & MacKerell, A. D., Jr. (2000). All-atom empirical force field for nucleic acids: I. Parameter optimization based on small molecule and condensed phase macromolecular target data. *Journal of Computational Chemistry*, 21, 86–104.
- Gao, J., Amara, P., Alhambra, C., & Field, M. J. (1998). A generalized hybrid orbital (GHO) method for the treatment of boundary atoms in combined QM/MM calculations. *Journal of Physical Chemistry A*, 102, 4714–4721.
- García-Viloca, M., Gao, J., Karplus, M., & Truhlar, D. G. (2004). How enzymes work: Analysis by modern rate theory and computer simulations. *Science*, 303, 186–195.
- Garst, A. D., Edwards, A. L., & Batey, R. T. (2011). Riboswitches: Structures and mechanisms. *Cold Spring Harbor Perspectives in Biology*, 3(6), a003533.
- Giambaşu, G. M., Lee, T.-S., Scott, W. G., & York, D. M. (2012). Mapping L1 ligase ribozyme conformational switch. *Journal of Molecular Biology*, 423(1), 106–122.
- Giambaşu, G. M., Lee, T.-S., Sosa, C. P., Robertson, M. P., Scott, W. G., & York, D. M. (2010). Identification of dynamical hinge points of the L1 ligase molecular switch. *RNA*, 16(4), 769–780.
- Giambaşu, G. M., Luchko, T., Herschlag, D., York, D. M., & Case, D. A. (2014). Ion counting from explicit-solvent simulations and 3D-RISM. *Biophysical Journal*, 106, 883–894.
- Giese, T. J., Chen, H., Huang, M., & York, D. M. (2014). Parametrization of an orbital-based linear-scaling quantum force field for noncovalent interactions. *Journal of Chemical Theory and Computation*, 10, 1086–1098.

- Giese, T. J., Huang, M., Chen, H., & York, D. M. (2014). Recent advances toward a general purpose linear-scaling quantum force field. *Accounts of Chemical Research*, 47, 2812–2820.
- Goh, G. B., Knight, J. L., & Brooks, C. L., III. (2012). Constant pH molecular dynamics simulations of nucleic acids in explicit solvent. *Journal of Chemical Theory and Computation*, 8, 36–46.
- Goh, G. B., Knight, J. L., & Brooks, C. L., III. (2013). Towards accurate prediction of protonation equilibrium of nucleic acids. *Journal of Physical Chemistry Letters*, 4(5), 760–766.
- Golden, B. L. (2011). Two distinct catalytic strategies in the hepatitis delta virus ribozyme cleavage reaction. *Biochemistry*, 50(44), 9424–9433.
- Golden, B. L., Hammes-Schiffer, S., Carey, P. R., & Bevilacqua, P. C. (2013). An integrated picture of HDV ribozyme catalysis. In R. Russell (Ed.), *Biophysics of RNA folding: Vol. 3* (pp. 135–167). New York: Springer.
- Gong, B., Chen, J.-H., Bevilacqua, P. C., Golden, B. L., & Carey, P. R. (2009). Competition between  $\text{Co}(\text{NH}_3)_6^{3+}$  and inner sphere  $\text{Mg}^{2+}$  ions in the HDV ribozyme. *Biochemistry*, 48, 11961–11970.
- Gong, B., Chen, J.-H., Chase, E., Chadalavada, D. M., Yajima, R., Golden, B. L., et al. (2007). Direct measurement of a  $\text{pK}_a$  near neutrality for the catalytic cytosine in the genomic HDV ribozyme using Raman crystallography. *Journal of the American Chemical Society*, 129, 13335–13342.
- Gong, B., Chen, J.-H., Yajima, R., Chen, Y., Chase, E., Chadalavada, D. M., et al. (2009). Raman crystallography of RNA. *Methods*, 49(2), 101–111.
- Gong, B., Chen, Y., Christian, E. L., Chen, J.-H., Chase, E., Chadalavada, D. M., et al. (2008). Detection of innersphere interactions between magnesium hydrate and the phosphate backbone of the HDV ribozyme using Raman crystallography. *Journal of the American Chemical Society*, 130, 9670–9672.
- Greenfeld, M., & Herschlag, D. (2009). Probing nucleic acid-ion interactions with buffer exchange-atomic emission spectroscopy. *Methods in Enzymology*, 469(10), 375–389.
- Grilley, D., Soto, A. M., & Draper, D. E. (2006).  $\text{Mg}^{2+}$ -RNA interaction free energies and their relationship to the folding of RNA tertiary structures. *Proceedings of the National Academy of Sciences of the United States of America*, 103(38), 14003–14008.
- Gu, H., Zhang, S., Wong, K.-Y., Radak, B. K., Dissanayake, T., Kellerman, D. L., et al. (2013). Experimental and computational analysis of the transition state for ribonuclease A-catalyzed RNA 2'-O-transphosphorylation. *Proceedings of the National Academy of Sciences of the United States of America*, 110, 13002–13007.
- Guttman, M., & Rinn, J. L. (2012). Modular regulatory principles of large non-coding RNAs. *Nature*, 482, 339–346.
- Hamelberg, D., Mongan, J., & McCammon, J. A. (2004). Accelerated molecular dynamics: A promising and efficient simulation method for biomolecules. *Journal of Chemical Physics*, 120, 11919–11929.
- Harris, M. E., & Cassano, A. G. (2008). Experimental analyses of the chemical dynamics of ribozyme catalysis. *Current Opinion in Chemical Biology*, 12, 626–639.
- Hashem, Y., & Auffinger, P. (2009). A short guide for molecular dynamics simulations of RNA systems. *Methods*, 47(3), 187–197.
- Heldenbrand, H., Janowski, P. A., Giambaşu, G., Giese, T. J., Wedekind, J. E., & York, D. M. (2014). Evidence for the role of active site residues in the hairpin ribozyme from molecular simulations along the reaction path. *Journal of the American Chemical Society*, 136, 7789–7792.
- Hengge, A. C. (2002). Isotope effects in the study of phosphoryl and sulfuryl transfer reactions. *Accounts of Chemical Research*, 35, 105–112.
- Herschlag, D. (1994). Ribonuclease revisited: Catalysis via the classical general acid-base mechanism or a triester-like mechanism? *Journal of the American Chemical Society*, 116(26), 11631–11635.

- Hoskins, A. A., & Moore, M. J. (2012). The spliceosome: A flexible, reversible macromolecular machine. *Trends in Biochemical Sciences*, 37(5), 179–188.
- Hou, G., & Cui, Q. (2013). Stabilization of different types of transition states in a single enzyme active site: QM/MM analysis of enzymes in the alkaline phosphatase superfamily. *Journal of the American Chemical Society*, 135, 10457–10469.
- Howard, J. J., Lynch, G. C., & Pettitt, B. M. (2011). Ion and solvent density distributions around canonical B-DNA from integral equations. *Journal of Physical Chemistry. B*, 115(3), 547–556.
- Ji, C. G., & Zhang, J. Z. H. (2011). Understanding the molecular mechanism of enzyme dynamics of ribonuclease A through protonation/deprotonation of HIS48. *Journal of the American Chemical Society*, 133, 17727–17737.
- Jorgensen, W. L., Maxwell, D. S., & Tirado-Rives, J. (1996). Development and testing of the OPLS all-atom force field on conformational energetics and properties of organic liquids. *Journal of the American Chemical Society*, 118, 11225–11236.
- Joung, I. S., & Cheatham, T. E., III. (2008). Determination of alkali and halide monovalent ion parameters for use in explicitly solvated biomolecular simulations. *Journal of Physical Chemistry. B*, 112, 9020–9041.
- Kaminski, G. A., Friesner, R. A., Tirado-Rives, J., & Jorgensen, W. L. (2001). Evaluation and reparametrization of the OPLS-AA force field for proteins via comparison with accurate quantum chemical calculations on peptides. *Journal of Physical Chemistry. B*, 105, 6474–6487.
- Ke, A., Zhou, K., Ding, F., Cate, J. H. D., & Doudna, J. A. (2004). A conformational switch controls hepatitis delta virus ribozyme catalysis. *Nature*, 429, 201–205.
- Kellerman, D. L., York, D. M., Piccirilli, J. A., & Harris, M. E. (2014). Altered (transition) states: mechanisms of solution and enzyme catalyzed RNA 2'-O-transphosphorylation. *Current Opinion in Chemical Biology*, 21, 96–102.
- Khandogin, J., & Brooks, C. L., III. (2005). Constant pH molecular dynamics with proton tautomerism. *Biophysical Journal*, 89, 141–157.
- Kirmizialtin, S., Silalahi, A. R. J., Elber, R., & Fenley, M. O. (2012). The ionic atmosphere around A-RNA: Poisson-Boltzmann and molecular dynamics simulations. *Biophysical Journal*, 102(4), 829–838.
- Klein, D. J., Been, M. D., & Ferré-D'Amaré, A. R. (2007). Essential role of an active-site guanine in glmS ribozyme catalysis. *Journal of the American Chemical Society*, 129(48), 14858–14859.
- Klingen, A. R., Bombarda, E., & Ullmann, G. M. (2006). Theoretical investigation of the behavior of titratable groups in proteins. *Photochemical & Photobiological Sciences*, 5, 588–596.
- Kovalenko, A., & Hirata, F. (2000). Potentials of mean force of simple ions in ambient aqueous solution. II. Solvation structure from the three-dimensional reference interaction site model approach, and comparison with simulations. *Journal of Chemical Physics*, 112(23), 10403.
- Kovalenko, A., Ten-no, S., & Hirata, F. (1999). Solution of three-dimensional reference interaction site model and hypernetted chain equations for simple point charge water by modified method of direct inversion in iterative subspace. *Journal of Computational Chemistry*, 20(9), 928–936.
- Kumar, S., Bouzida, D., Swendsen, R. H., Kollman, P. A., & Rosenberg, J. M. (1992). The weighted histogram analysis method for free-energy calculations on biomolecules. I. The method. *Journal of Computational Chemistry*, 13, 1011–1021.
- Laio, A., & Parrinello, M. (2002). Escaping free-energy minima. *Proceedings of the National Academy of Sciences of the United States of America*, 99, 12562–12566.
- Lassila, J. K., Zalatan, J. G., & Herschlag, D. (2011). Biological phosphoryl-transfer reactions: Understanding mechanism and catalysis. *Annual Review of Biochemistry*, 80, 669–702.

- Lee, M. S., Salsbury, F. R., Jr., & Brooks, C. L., III. (2004). Constant-pH molecular dynamics using continuous titration coordinates. *Proteins*, *56*, 738–752.
- Lee, T.-S., Giambaşu, G. M., Harris, M. E., & York, D. M. (2011). Characterization of the structure and dynamics of the HDV ribozyme in different stages along the reaction path. *Journal of Physical Chemistry Letters*, *2*(20), 2538–2543.
- Lee, T.-S., Giambaşu, G. M., Sosa, C. P., Martick, M., Scott, W. G., & York, D. M. (2009). Threshold occupancy and specific cation binding modes in the hammerhead ribozyme active site are required for active conformation. *Journal of Molecular Biology*, *388*, 195–206.
- Lee, T.-S., Giambaşu, G. M., & York, D. M. (2010). Insights into the role of conformational transitions and metal ion binding in RNA catalysis from molecular simulations. In R. A. Wheeler (Ed.), *Annual reports in computational chemistry* (Vol. 6, pp. 169–200): Amsterdam, The Netherlands: Elsevier.
- Lee, T.-S., Radak, B. K., Huang, M., Wong, K.-Y., & York, D. M. (2014). Roadmaps through free energy landscapes calculated using the multidimensional vFEP approach. *Journal of Chemical Theory and Computation*, *10*, 24–34.
- Lee, T.-S., Radak, B. K., Pabis, A., & York, D. M. (2013). A new maximum likelihood approach for free energy profile construction from molecular simulations. *Journal of Chemical Theory and Computation*, *9*, 153–164.
- Lee, T.-S., Silva Lopez, C., Giambaşu, G. M., Martick, M., Scott, W. G., & York, D. M. (2008). Role of  $Mg^{2+}$  in hammerhead ribozyme catalysis from molecular simulation. *Journal of the American Chemical Society*, *130*(10), 3053–3064.
- Lee, T.-S., Wong, K.-Y., Giambaşu, G. M., & York, D. M. (2013). Bridging the gap between theory and experiment to derive a detailed understanding of hammerhead ribozyme catalysis. In G. A. Soukup (Ed.), *Progress in Molecular Biology and Translational Science: Vol. 120* (pp. 25–91). London, UK: Elsevier, Academic Press.
- Lee, T.-S., & York, D. M. (2008). Origin of mutational effects at the C3 and G8 positions on hammerhead ribozyme catalysis from molecular dynamics simulations. *Journal of the American Chemical Society*, *130*(23), 7168–7169.
- Lee, T.-S., & York, D. M. (2010). Computational mutagenesis studies of hammerhead ribozyme catalysis. *Journal of the American Chemical Society*, *132*(38), 13505–13518.
- Lévesque, D., Reymond, C., & Perreault, J.-P. (2012). Characterization of the trans Watson-Crick GU base pair located in the catalytic core of the antigenomic HDV ribozyme. *PLoS One*, *7*(6), 40309.
- Li, P., & Merz, K. M., Jr. (2014). Taking into account the ion-induced dipole interaction in the nonbonded model of ions. *Journal of Chemical Theory and Computation*, *10*, 289–297.
- Li, P., Roberts, B. P., Chakravorty, D. K., & Merz, K. M., Jr. (2013). Rational design of particle mesh Ewald compatible Lennard-Jones parameters for +2 metal cations in explicit solvent. *Journal of Chemical Theory and Computation*, *9*, 2733–2748.
- Lilley, D. M. J. (2005). Structure, folding and mechanisms of ribozymes. *Current Opinion in Structural Biology*, *15*, 313–323.
- Lilley, D. M. J. (2011). Catalysis by the nucleolytic ribozymes. *Biochemical Society Transactions*, *39*, 641–646.
- Lilley, D. M. J. (2011). Mechanisms of RNA catalysis. *Philosophical Transactions of the Royal Society B*, *366*, 2910–2917.
- Link, K. H., & Breaker, R. R. (2009). Engineering ligand-responsive gene-control elements: Lessons learned from natural riboswitches. *Gene Therapy*, *16*, 1189–1201.
- Lodola, A., & Mulholland, A. J. (2013). Computational enzymology. In L. Monticelli & E. Salonen (Eds.), *Biomolecular simulations: Vol. 924* (pp. 67–89). New York, NY: Humana Press.
- Luchko, T., Gusarov, S., Roe, D. R., Simmerling, C., Case, D. A., Tuszynski, J., & Kovalenko, A. (2010). Three-dimensional molecular theory of solvation coupled with molecular dynamics in AMBER. *Journal of Chemical Theory and Computation*, *6*, 607–624.

- MacKerell, A. D., Jr., & Banavali, N. K. (2000). All-atom empirical force field for nucleic acids: II. *Application to molecular dynamics simulations of DNA and RNA in solution. Journal of Computational Chemistry*, *21*, 105–120.
- Martick, M., Lee, T.-S., York, D. M., & Scott, W. G. (2008). Solvent structure and hammerhead ribozyme catalysis. *Chemistry & Biology*, *15*, 332–342.
- Martínez, J. M., Pappalardo, R. R., & Marcos, E. S. (1999). First-principles ion–water interaction potentials for highly charged monatomic cations. Computer simulations of  $\text{Al}^{3+}$ ,  $\text{Mg}^{2+}$ , and  $\text{Be}^{2+}$  in water. *Journal of the American Chemical Society*, *121*, 3175–3184.
- Maruyama, Y., Yoshida, N., & Hirata, F. (2010). Revisiting the salt-induced conformational change of DNA with 3D-RISM theory. *Journal of Chemical Physics B*, *114*(19), 6464–6471.
- McDowell, S. E., Špačková, N., Šponer, J., & Walter, N. G. (2006). Molecular dynamics simulations of RNA: An in silico single molecule approach. *Biopolymers*, *85*, 169–184.
- Meier-Schellersheim, M., Fraser, I. D. C., & Klauschen, F. (2009). Multiscale modeling for biologists. Wiley Interdisciplinary Reviews. *Systems Biology and Medicine*, *1*(1), 4–14.
- Misra, V. K., & Draper, D. E. (1998). On the role of magnesium ions in RNA stability. *Biopolymers*, *48*, 113–135.
- Misra, V. K., & Draper, D. E. (2002). The linkage between magnesium binding and RNA folding. *Journal of Molecular Biology*, *317*, 507–521.
- Mongan, J., Case, D. A., & McCammon, J. A. (2004). Constant pH molecular dynamics in generalized Born implicit solvent. *Journal of Computational Chemistry*, *25*, 2038–2048.
- Murray, J. B., Dunham, C. M., & Scott, W. G. (2002). A pH-dependent conformational change, rather than the chemical step, appears to be rate-limiting in the hammerhead ribozyme cleavage reaction. *Journal of Molecular Biology*, *315*, 121–130.
- Nakajima, N., Nakamura, H., & Kidera, A. (1997). Multicanonical ensemble generated by molecular dynamics simulation for enhanced conformational sampling of peptides. *Journal of Physical Chemistry. B*, *101*, 817–824.
- Nakano, S., Chadalavada, D. M., & Bevilacqua, P. C. (2000). General acid–base catalysis in the mechanism of a hepatitis delta virus ribozyme. *Science*, *287*, 1493–1497.
- Nakano, S., Proctor, D. J., & Bevilacqua, P. C. (2001). Mechanistic characterization of the HDV genomic ribozyme: Assessing the catalytic and structural contributions of divalent metal ions within a multichannel reaction mechanism. *Biochemistry*, *40*, 12022–12038.
- Nam, K., Cui, Q., Gao, J., & York, D. M. (2007). Specific reaction parametrization of the AM1/d Hamiltonian for phosphoryl transfer reactions: H, O, and P atoms. *Journal of Chemical Theory and Computation*, *3*, 486–504.
- Nam, K., Gao, J., & York, D. (2008). Electrostatic interactions in the hairpin ribozyme account for the majority of the rate acceleration without chemical participation by nucleobases. *RNA*, *14*, 1501–1507.
- Nam, K., Gao, J., & York, D. M. (2008). Quantum mechanical/molecular mechanical simulation study of the mechanism of hairpin ribozyme catalysis. *Journal of the American Chemical Society*, *130*(14), 4680–4691.
- Nixon, P. L., & Giedroc, D. P. (2000). Energetics of a strongly pH dependent RNA tertiary structure in a frameshifting pseudoknot. *Journal of Molecular Biology*, *296*, 659–671.
- Onufriev, A., Bashford, D., & Case, D. A. (2004). Exploring protein native states and large-scale conformational changes with a modified generalized Born model. *Proteins*, *55*, 383–394.
- Oostenbrink, C., Villa, A., Mark, A. E., & van Gunsteren, W. F. (2004). A biomolecular force field based on the free enthalpy of hydration and solvation: The GROMOS force-field parameter sets 53A5 and 53A6. *Journal of Computational Chemistry*, *25*, 1656–1676.
- Pabit, S. A., Meisburger, S. P., Li, L., Blose, J. M., Jones, C. D., & Pollack, L. (2010). Counting ions around DNA with anomalous small-angle X-ray scattering. *Journal of the American Chemical Society*, *132*(46), 16334–16336.

- Pabit, S. A., Qiu, X., Lamb, J. S., Li, L., Meisburger, S. P., & Pollack, L. (2009). Both helix topology and counterion distribution contribute to the more effective charge screening in dsRNA compared with dsDNA. *Nucleic Acids Research*, *37*(12), 3887–3896.
- Panteva, M. T., Giambaşu, G. M., & York, D. M. (n.d.). Comparison of structural, thermodynamic, kinetic and mass transport properties of  $Mg^{2+}$  ion models commonly used in biomolecular simulations. *Journal of Computational Chemistry*, in press.
- Penchovsky, R. (2014). Computational design of allosteric ribozymes as molecular biosensors. *Biotechnology Advances*, *32*, 1015–1027.
- Pérez, A., Luque, F. J., & Orozco, M. (2011). Frontiers in molecular dynamics simulations of DNA. *Accounts of Chemical Research*, *45*, 196–205.
- Pérez, A., Marchán, I., Svozil, D., Sponer, J., Cheatham, T. E., III, Laughton, C. A., & Orozco, M. (2007). Refinement of the AMBER force field for nucleic acids: Improving the description of  $\alpha/\gamma$  conformers. *Biophysical Journal*, *92*, 3817–3829.
- Pollack, L. (2011). SAXS studies of ion-nucleic acid interactions. *Annual Review of Biophysics*, *40*, 225–242.
- Ponder, J. W., Wu, C., Ren, P., Pande, V. S., Chodera, J. D., Schnieders, M. J., et al. (2010). Current status of the AMOEBA polarizable force field. *Journal of Physical Chemistry. B*, *114*, 2549–2564.
- Quirk, D. J., & Raines, R. T. (1999). His ... Asp catalytic dyad of ribonuclease A: Histidine pKa values in the wild-type, D121N, and D121A enzymes. *Biophysical Journal*, *76*, 1571–1579.
- Raines, R. T. (1998). Ribonuclease A. *Chemical Reviews*, *98*, 1045–1065.
- Reuter, N., Dejaegere, A., Maigret, B., & Karplus, M. (2000). Frontier bonds in QM/MM methods: A comparison of different approaches. *Journal of Physical Chemistry A*, *104*, 1720–1735.
- Rhodes, M. M., Réblová, K., Sponer, J., & Walter, N. G. (2006). Trapped water molecules are essential to structural dynamics and function of a ribozyme. *Proceedings of the National Academy of Sciences of the United States of America*, *103*, 13380–13385.
- Roth, A., & Breaker, R. R. (2009). The structural and functional diversity of metabolite-binding riboswitches. *Annual Review of Biochemistry*, *78*, 305–334.
- Rueda, M., Cubero, E., Laughton, C. A., & Orozco, M. (2004). Exploring the counterion atmosphere around DNA: What can be learned from molecular dynamics simulations? *Biophysical Journal*, *87*, 800–811.
- Salomon-Ferrer, R., Götz, A. W., Poole, D., Le Grand, S., & Walker, R. C. (2013). Routine microsecond molecular dynamics simulations with AMBER on GPUs. 2. Explicit solvent particle mesh Ewald. *Journal of Chemical Theory and Computation*, *9*, 3878–3888.
- Schmeing, T. M., & Ramakrishnan, V. (2009). What recent ribosome structures have revealed about the mechanism of translation. *Nature*, *461*(7268), 1234–1242.
- Scott, W. G. (2007). Ribozymes. *Current Opinion in Structural Biology*, *17*, 280–286.
- Senn, H. M., & Thiel, W. (2009). QM/MM methods for biomolecular systems. *Angewandte Chemie International Edition*, *48*, 1198–1229.
- Sharp, P. A. (2009). The centrality of RNA. *Cell*, *136*(4), 577–580.
- Sherwood, P., Brooks, B. R., & Sansom, M. S. P. (2008). Multiscale methods for macromolecular simulations. *Current Opinion in Structural Biology*, *18*(5), 630–640.
- Shirts, M. R., & Chodera, J. D. (2008). Statistically optimal analysis of samples from multiple equilibrium states. *Journal of Chemical Physics*, *129*, 124105.
- Souaille, M., & Roux, B. (2001). Extension to the weighted histogram analysis method: Combining umbrella sampling with free energy calculations. *Computer Physics Communications*, *135*, 40–57.
- Suess, B., & Weigand, J. E. (2008). Engineered riboswitches: Overview, problems and trends. *RNA Biology*, *5*, 1–6.

- Sugita, Y., Kitao, A., & Okamoto, Y. (2000). Multidimensional replica-exchange method for free-energy calculations. *Journal of Chemical Physics*, *113*, 6042–6051.
- Tan, Z., Gallicchio, E., Lapelosa, M., & Levy, R. M. (2012). Theory of binless multi-state free energy estimation with applications to protein-ligand binding. *Journal of Chemical Physics*, *136*, 144102.
- Thomas, A. S., & Elcock, A. H. (2006). Direct observation of salt effects on molecular interactions through explicit-solvent molecular dynamics simulations: Differential effects on electrostatic and hydrophobic interactions and comparisons to Poisson-Boltzmann theory. *Journal of the American Chemical Society*, *128*, 7796–7806.
- Torelli, A. T., Krucinska, J., & Wedekind, J. E. (2007). A comparison of vanadate to a 2'-5' linkage at the active site of a small ribozyme suggests a role for water in transition-state stabilization. *RNA*, *13*, 1052–1070.
- Torrie, G. M., & Valleau, J. P. (1974). Monte Carlo free energy estimates using non-Boltzmann sampling: Application to the sub-critical Lennard-Jones fluid. *Chemical Physics Letters*, *28*, 578–581.
- Torrie, G. M., & Valleau, J. P. (1977). Nonphysical sampling distributions in Monte Carlo free-energy estimation: Umbrella sampling. *Journal of Computational Physics*, *23*, 187–199.
- Ullmann, G. M. (2003). Relations between protonation constants and titration curves in polyprotic acids: A critical view. *Journal of Physical Chemistry. B*, *107*, 1263–1271.
- Valadkhan, S. (2010). Role of the snRNAs in spliceosomal active site. *RNA Biology*, *7*(3), 345–353.
- Valleau, J. P., & Card, D. N. (1972). Monte Carlo estimation of the free energy by multistage sampling. *Journal of Chemical Physics*, *57*, 5457–5462.
- van der Kamp, M. W., & Mulholland, A. J. (2013). Combined quantum mechanics/molecular mechanics (QM/MM) methods in computational enzymology. *Biochemistry*, *52*, 2708–2728.
- Vanden-Eijnden, E. (2009). Some recent techniques for free energy calculations. *Journal of Computational Chemistry*, *30*(11), 1737–1747.
- Viladoms, J., Scott, L. G., & Fedor, M. J. (2011). An active-site guanine participates in glmS ribozyme catalysis in its protonated state. *Journal of the American Chemical Society*, *133*(45), 18388–18396.
- Wadkins, T. S., Shih, I., Perrotta, A. T., & Been, M. D. (2001). A pH-sensitive RNA tertiary interaction affects self-cleavage activity of the HDV ribozymes in the absence of added divalent metal ion. *Journal of Molecular Biology*, *305*, 1045–1055.
- Walter, N. G. (2007). Ribozyme catalysis revisited: Is water involved? *Molecular Cell*, *28*, 923–929.
- Wang, J., Cieplak, P., & Kollman, P. A. (2000). How well does a restrained electrostatic potential (RESP) model perform in calculating conformational energies of organic biological molecules. *Journal of Computational Chemistry*, *21*(12), 1049–1074.
- Warshel, A., & Levitt, M. (1976). Theoretical studies of enzymic reactions: Dielectric, electrostatic and steric stabilization of the carbonium ion in the reaction of lysozyme. *Journal of Molecular Biology*, *103*, 227–249.
- Wilcox, J. L., Ahluwalia, A. K., & Bevilacqua, P. C. (2011). Charged nucleobases and their potential for RNA catalysis. *Accounts of Chemical Research*, *44*, 1270–1279.
- Wilson, D. N., & Cate, J. H. D. (2012). The structure and function of the eukaryotic ribosome. *Cold Spring Harbor Perspectives in Biology*, *4*(5), a011536.
- Wilson, T. J., Li, N.-S., Lu, J., Frederiksen, J. K., Piccirilli, J. A., & Lilley, D. M. J. (2010). Nucleobase-mediated general acid-base catalysis in the Varkud satellite ribozyme. *Proceedings of the National Academy of Sciences of the United States of America*, *107*, 11751–11756.
- Wilson, T. J., & Lilley, D. M. J. (2009). The evolution of ribozyme chemistry. *Science*, *323*(5920), 1436–1438.

- Wojtas-Niziurski, W., Meng, Y., Roux, B., & Bernèche, S. (2013). Self-learning adaptive umbrella sampling method for the determination of free energy landscapes in multiple dimensions. *Journal of Chemical Theory and Computation*, 9(4), 1885–1895.
- Wong, K.-Y., Gu, H., Zhang, S., Piccirilli, J. A., Harris, M. E., & York, D. M. (2012). Characterization of the reaction path and transition states for RNA transphosphorylation models from theory and experiment. *Angewandte Chemie International Edition*, 51, 647–651.
- Wong, K.-Y., Lee, T.-S., & York, D. M. (2011). Active participation of the  $Mg^{2+}$  ion in the reaction coordinate of RNA self-cleavage catalyzed by the hammerhead ribozyme. *Journal of Chemical Theory and Computation*, 7(1), 1–3.
- Wong, K.-Y., & York, D. M. (2012). Exact relation between potential of mean force and free-energy profile. *Journal of Chemical Theory and Computation*, 8(11), 3998–4003.
- Wu, X., & Brooks, B. R. (2012). Efficient and unbiased sampling of biomolecular systems in the canonical ensemble: A review of self-guided Langevin dynamics. *Advances in Chemical Physics*, 150, 255–326.
- Xie, W., Orozco, M., Truhlar, D. G., & Gao, J. (2009). X-Pol potential: An electronic structure-based force field for molecular dynamics simulation of a solvated protein in water. *Journal of Chemical Theory and Computation*, 5, 459–467.
- Yonetani, Y., Maruyama, Y., Hirata, F., & Kono, H. (2008). Comparison of DNA hydration patterns obtained using two distinct computational methods, molecular dynamics simulation and three-dimensional reference interaction site model theory. *Journal of Chemical Physics*, 128, 185102.
- Yoo, J., & Aksimentiev, A. (2012). Competitive binding of cations to duplex DNA revealed through molecular dynamics simulations. *Journal of Physical Chemistry. B*, 116(43), 12946–12954.
- York, D. M., & Lee, T.-S. (Eds.), (2009). *Multiscale quantum models for biocatalysis: Modern techniques and applications*. New York: Springer.
- Zgarbová, M., Otyepka, M., Šponer, J., Mládek, A., Banáš, P., Cheatham, T. E., III, & Jurečka, P. (2011). Refinement of the Cornell et al. nucleic acids force field based on reference quantum chemical calculations of glycosidic torsion profiles. *Journal of Chemical Theory and Computation*, 7, 2886–2902.
- Zhang, S., Gu, H., Chen, H., Strong, E., Liang, D., Dai, Q., Harris, M. E. (n.d.). An associative two metal ion mechanism for non-enzymatic RNA 2'-O-transphosphorylation. *Nature Chemistry*, submitted.
- Zhang, Y., Lee, T.-S., & Yang, W. (1999). A pseudobond approach to combining quantum mechanical and molecular mechanical methods. *Journal of Chemical Physics*, 110, 46–54.
- Zuckerman, D. M. (2011). Equilibrium sampling in biomolecular simulations. *Annual Review of Biophysics*, 40, 41–62.
- Zwier, M. C., & Chong, L. T. (2010). Reaching biological timescales with all-atom molecular dynamics simulations. *Current Opinion in Pharmacology*, 10, 745–752.